Contribution of volcanism to the initiation of plague pandemics

FELL, HENRY,GILLIES

Contribution of volcanism to the initiation of plague pandemics

by

Henry Gillies Fell

Thesis

For the degree of

Master of Science by Research

Department of Earth Sciences
Durham University
2017

Abstract

The *Yersinia pestis* bacterium is responsible for the three major plague pandemics of the Common Era, cumulatively responsible for hundreds of millions of deaths and huge societal impacts. Factors influencing the initiation of plague pandemics are still controversial amongst scientists and historians. However recent advances in DNA sequencing and recovery, and ecological and epidemiological modelling, have provided new information regarding the evolution of *Y. pestis* and the potential influence of climate upon pandemic episodes respectively. Rapid bursts in genetic fixation rates and evolutionary divergences were identified preceding the initiation of the Black Death and Third Pandemic, and climatic factors are now accepted as a key influence upon plague prevalence over an annual to centennial timescale. By reassessing climatic perturbations prior to major pandemics and utilising recent satellite data this thesis suggests a mechanistic pathway linking explosive high sulphur and halogen eruptions within periods of sustained elevated global volcanic forcing, to evolutionary and epidemiological progression of *Y. pestis*. The periods of global volcanic forcing coincident with pandemic episodes are shown to do the following: (1) increase levels of a known mutagenic element in an area proposed as a source of diversity within the *Y. pestis* genome through a novel and previously unexplored mechanism and, (2) contribute to regional climatic shifts fully coincident with the timing and distribution of plague immediately preceding pandemic initiation. The volcanic influence suggested not only represents an alternate hypothesis for the genetic expansion and subsequent pandemic impact of plague but also illustrates a previously unexplored risk following large explosive volcanic eruptions.

Even if you win, you're still a rat.

Sam Carter

Contents

Acknowledgements

Huge thanks have to go to James Baldini and Ben Dodds. Initially for allowing me to begin research on a completely different topic of my choice. They both supported me in my efforts to determine if Pilot Whale hunting records from the Faroe Islands represented a proxy for climatic changes in the North Atlantic. It turns out they did, but someone had already published a paper within this field far beyond what I could achieve in a year. I then started work on their preferred subject, looking into the influence the 1257 C.E. Samalas eruption could have had upon the Black Death pandemic. The discussions we had around this topic were eye opening and my first experience of working as part of an inter-disciplinary team, which is something I now hope to continue. Thanks to Ben for providing invaluable historic knowledge of the Black Death and regularly pointing me in the right direction. Thanks to James for putting up with my near endless questions and helping to streamline the project and drive it forward. Without their guidance and support I would not have even considered this topic of research, which I am now happy to be continuing for the next 3 years through PhD study.

Thanks also have to go to Gary Sharples for aiding on the biological side of the project and confirming that our ideas were not completely implausible, and Andrew Millard for furthering my limited understanding of dendrochronology. Rob Wilson deserves further thanks for aiding in the initial stages of my project and providing helpful feedback at EGU. Thanks also have to go to Kathleen Pribyl for her expert advice in the latter stages of the project.

Further thanks to Emma Gregory for providing the script that allowed the extraction of calibration temperatures within the source and zoonosis area and Erin Scott for putting up with incessant questions.

Thanks all.

Chapter 1: Introduction

Yersinia pestis is the bacterial agent of plague responsible for three major plague pandemics within the Common Era which influenced global population and societal change for centuries after pandemic initiation[1-3]. Plague is currently listed as a re-emergent disease due to the increase in reported cases, primarily in Africa, due to expanding wild animal host populations[4]. Plague is therefore still a relevant, 'modern' disease and comprehensively understanding plague dynamics is essential to mitigating potential, and substantial, future risk [4,5] .

Y. pestis is capable of three forms of primary infection, bubonic, septicemic and pneumonic. Bubonic plague is the most common *Y. pestis* infection route and occurs through regurgitation of an infected blood meal by a vector such as a flea or louse[6] after biting the host. The bacterium is then transmitted via the host's lymphatics to the lymph nodes causing painful inflammations, termed 'buboes'[7]. The mortality rate is between 40% and 70% but is significantly reduced through antibiotic use[8]. Septicemic plague is similar to bubonic however the bacteria are transmitted through the circulatory system and this type of plague results in a higher mortality rate than bubonic plague, with death predominantly caused by sepsis. Septicemic plague either follows initial infection via bubonic or pneumonic infection (i.e., a secondary infection) or less commonly (up to 30% of cases) can develop following an infected flea bite but with no presence of alternate infection (a primary infection)[9-11]. Pneumonic plague is aerosol borne and causes rapid fulminant pneumonic infection in the lungs resulting in intense coughing and fever and has fatality rates near 100% if untreated[12,13].

Y. pestis was first isolated in 1894 coincident with plague's arrival in Hong Kong in the Third Pandemic[14] (1850 C.E. onwards[15]) and is now further confirmed as responsible for the Justinian Plague (540 C.E. through the eighth century[16]) and the pandemic episode that initiated at the Black Death (1338 C.E. through the seventeenth century[17,18]) through genetic analysis of ancient DNA (aDNA) recovered from plague grave sites[19,20]. Increasing aDNA data and isolation of extant strains from current host populations and patients have recently enabled increased investigation into the evolutionary pathway of *Y. pestis*. *Y. pestis*

may have diverged from its most recent common ancestor (MRCA) *Yersinia pseudotuberculosis* 53,000 years ago[21] and now has near global coverage across five genetically distinct branches[22]. Rasmussen et al. (2015)[21] suggest that early strains were endemic in isolated areas across Eurasia however *Y. pestis* only developed bubonic capability roughly three thousand years ago following progressive genetic losses. The Justinian Plague, the first major plague pandemic, was associated with a now extinct strain from a possible Central Asian source[23], however earlier references suggested an alternate source from East Africa[1,24]. The subsequent two pandemics were both preceded by diversification events identified by polytomies (apparent instantaneous diversification resulting in greater than two descendants) and a rapid increase in fixation rate (fixation is when the frequency of a new gene reaches 100% within a population)[22]. The diversification event that immediately preceded the Black Death (the diversification event termed the 'Big Bang') gave rise to four new genetic branches of *Y. pestis*[22], with the strain responsible for the pandemic basal to Branch 1. The Third Pandemic and its associated prior diversification gave rise to the 1.ORI group[25] which now has global distribution due to the extensive transmission through international shipping routes during this latest pandemic episode[26]. Cui et al. (2013)[22] suggest that these diversification events were caused by the increase in replication cycles during epidemic episodes. However they also state that "host density changes driven by climatic factors" cannot be excluded as a potential causational factor of events.

Y. pestis is usually maintained in rodent populations. However several other mammals such as prairie dogs, guinea pigs, camels and cats can also harbour the bacterium[4]. No permanent plague foci are currently extant in Western Europe and the potential existence of one during pandemic episodes is still debated[20]. Plague foci are currently found globally between northern and southern 20°C summer isotherms following the transmission of Third Pandemic[15], however the largest concentration of species is found in the historic source region of Central Asia[27]. Davis et al. (2004)[28] completed the seminal investigation of plague within the great gerbil (*Rhombomys opimus*) populations native to the Balkhash area of Kazakhstan, utilising extensive field data collected from 1955 C.E to

1996 C.E. to estimate host and vector densities. This study suggested that thresholds of susceptible hosts and total host populations determined the initiation and persistence of *Y. pestis* infection respectively within this wild population, with a one to two year lag[28]. Several studies have since suggested that host and vector densities within this area are influenced by climate, and that specific climatic conditions may drive increased plague risk both within host populations and local human populations[29-31]. Through the complete period of data collection (1949-1995 C.E.), warm spring times and wet summers correlate with increased plague risk due to their positive influence on host and vector densities[29]. Over longer timescales, including historic plague pandemics, warm and wet conditions coincide with major pandemic episodes in this area. This supports the concept that climate may have influenced plague prevalence during these periods[5]. Studies from this region are only representative of a small study area (roughly 2% of Kazakhstan[5]), however the conditions coinciding with historic pandemic episodes and plague studies from other localities suggest climatic factors may influence plague through the 'trophic cascade' mechanism[32,33]. This mechanism suggests an increase in primary productivity, in this case driven by climatic factors, which leads to an increase in host rodent species due to greater abundances of food sources. Larger host populations can therefore support larger vector populations, which consequently increases plague prevalence and eventually the potential risk of transmission to human populations (zoonosis). The warm and wet conditions identified as potentially important in the initiation of pandemic episodes are expected to become more prevalent across Central Asian source regions in the future because of anthropogenic climate change[5].

If one accepts that climate change is key to initiating plague pandemics, the question then becomes 'what influenced the climate leading to a pandemic?'. Volcanism regularly influenced climate and subsequently societal development throughout the Common Era on a global scale[34-36]. Previously, Stothers et al. (1999)[37] observed that volcanism regularly correlated with periods of 'pandemic' across Europe and the Middle East[37]. Volcanic induced global cooling following sufficiently large eruptions correlates with periods of poor harvests and famine[38-40] as observed following the 1815 C.E. Tambora eruption[34,41].

Malnutrition negatively influences human immunity[42] and therefore could exacerbate a pandemic episode, however this observation is not specific to *Y. pestis* and consequently the volcanic influence on plague pandemics remains unknown.

Several studies have suggested a link between volcanism and the Justinian Plague[1,24,43]. The early sixth century was a period with abundant volcanic eruptions, identified both through the nature of reconstructed climatic impacts[37,43], sulphur spikes within ice cores (536 C.E. Northern Hemisphere eruption, -11.3 (Wm^{-2}) Global volcanic forcing (GVF); 540 C.E. Tropical eruption, -19.14 (Wm^{-2}) GVF)[44], and historical accounts of volcanic dry fogs across Europe in 536 C.E.[37]. These eruptions combined with a further tropical eruption in 547 C.E. may have induced a globally recognised cool period extending from 540 to 660 C.E., known as the Late Antiquities Little Ice Age or LALIA[43]. This cooling was potentially sustained through positive sea ice ocean feedbacks[43] previously hypothesised to link intense and sustained thirteenth century volcanism to the Little Ice Age (LIA)[45]. The first record of Justinian Plague fatalities are from the relatively small Egyptian city of Pelusium in 540 C.E. after which *Y. pestis* spread to the port city of Alexandria and from there throughout the Mediterranean[1]. Recent genetic evidence from Justinian Plague grave sites suggest the *Y. pestis* strain responsible is now extinct, and that it initially diverged genetically from Central Asian strains[23]. Rasmussen et al. (2015)[21] suggest this newly discovered strain diverged around 4 C.E. (95% Highest Posterior Density (HPD) interval, 400 B.C.E. – 315 C.E.), roughly five centuries prior to the initiation of the Justinian Plague. Plague has been hypothesised to have spread up the Nile during the volcanically cooled period, through the normally intolerable heat of the Sahara from a potential East African source region in the Kingdom of Aksum (Ethiopia)[1,24,46]. Transmission of *Y. pestis* from Central Asia to East Africa would have been necessary between the divergence of the strain and the Justinian Plague to incorporate the theory of an African genesis with the identified source region.

The 1257 C.E. Samalas eruption was the largest single sulphate injection of the Common Era as recorded in bi-polar ice cores[44]. However, its climatic influence is debated due to regular discordance between model predictions and proxy records[47]. The Northern

Hemisphere exhibits heterogeneous cooling following the Samalas eruption with Western Europe, Japan and Siberia cooling intensely while North America experienced minor warming[39]. The Samalas eruption coincides with a period of further large eruptions in the late thirteenth century which may have contributed to the initiation of the LIA[45]. Other than Stothers et al.'s (2000)[38] reference to 'pestilence' across Europe in 1259 C.E. and 'plague' in the Middle East in 1258 C.E. (neither of which is a proven true *Y. pestis* plague), Samalas' influence on plague is occasionally discussed but generally dismissed[3].

Large explosive eruptions are hypothesised to have a deleterious effect on global ozone through the stratospheric injection of sulphur dioxide (SO_2) and halogen species, primarily chlorine[39] which catalyse ozone destruction. This effect was observed following the 1991 C.E. Pinatubo eruption[48]. However due to the limited transmission of chlorine to the stratosphere[49], it was observed that ozone depletion must have been aided considerably by anthropogenic chlorine[50,51]. Recent studies and primary observations have however suggested that chlorine is capable of stratospheric injection following a volcanic eruption therefore implying that pre-industrial eruptions such as Samalas and Tambora could have influenced ozone levels. Gullet et al. (2017)[39] recently suggested that Samalas may have had a significant and rapid destructive impact on ozone levels in the years following the 1257 C.E. eruption.

Ozone absorbs incident ultraviolet radiation and therefore mediates surface radiation of potentially harmful wavelengths such as UV-B (λ = 290-320nm)[52]. Elevated UV-B levels are known to cause protein and DNA damage and can cause skin cancer in humans, reduced larval survival in amphibians, modified plant morphology and altered bacterial diversity[53]. Increased UV-B values may also influence evolutionary events through geological time, contributing to rapid diversification within particular species, both through volcanically mediated ozone depletion and alternate methods of UV-B fluctuation[54-57]. Both the 1257 C.E. Samalas eruption and the 1815 C.E Tambora eruption are within roughly a decade of polytomy (apparently instantaneous diversifications resulting in more than two descendants) estimates warranting further analysis of the potential influence of these volcanic events on *Y. pestis.*

Polytomies identified through the molecular clock method may represent several other events aside from a rapid divergence event which must be acknowledged and discussed. Cui et al. 2013[58] suggest that the polytomies identified in *Y. pestis* represent 'starburst genealogies' when multiple genealogies diverge from a single ancestor. However, this may reflect insufficient data, as intermediate branch points have not been identified. Incomplete linage sorting or 'deep coalescence'[59] could also contribute to apparent polytomies when genetic divergence occurs prior to speciation and could therefore produce an apparent rapid genetic diversification. Assuming however that the polytomy identified does represent a true rapid genetic expansion it follows that, as Cui et al.[58] suggested, this may have been caused by historic epidemics, when the population and hence multiplication cycles of *Y. pestis* rapidly increase. Synthesis of this with modern ecological research, suggesting synchrony of climatic variation and plague cycles[5,28,60] would suggest that the polytomy dates hypothesised should coincide with conditions preferable for increased plague prevalence. This study however finds potentially beneficial climatic conditions to have occured significantly after these diversification events suggesting either: (1) the polytomy dates are overestimates or potentially erroneous, which is plausible given the uncertainties inherent in the method[23] or, (2) the diversification identified was influenced by an event independent of *Y. pestis* population dynamics, which is further explored with regards to volcanism.

To reassess the potential impact prolonged periods of large scale explosive volcanism may have upon plague pandemics this thesis analyses the post-volcanism climate change and societal responses across areas identified as pivotal to the initiation of plague – particularly the Black Death pandemic. This thesis further explores a novel hypothesis relating explosive halogen and sulphur rich eruptions with rapid developments of *Y. pestis* prior to the two most recent pandemic episodes.

The key areas of investigation includes Central and East Asia, extending from the South China Sea in the South East to Kazakhstan in the North West. This area encompasses hypothesized source regions of *Y. pestis* for each pandemic episode[15,23,58] and is covered by recent high (spatial and temporal) resolution climatic reconstructions

across the appropriate time intervals[61-63]. Radiative reconstructions are also possible across this area through global radiative (Erythemal UV-B) data[53] which is discussed in comparison to two of the largest volcanic eruptions of the Common Era.

The core objectives of this study are to analyse climatic and radiative reconstructions following extremely high sulphate and halogen eruptions within periods of prolonged volcanism coincident with plague pandemic episodes. Key areas of investigation are how volcanism may impact factors across the broad plague nexus including: (1) microbial evolution, (2) host and vector population dynamics, and (3) human population health.

Chapter 2: Plague Background

2.1: Plague in the modern context

Plague is predominantly considered as a historic disease, most well-known for the Black Death pandemic which devastated Eurasian populations in the fourteenth century and persisted in isolated areas until the seventeenth century[2,3]. Plague is currently categorised as a re-emergent disease by the World Health Organisation (WHO) due to its increasing prevalence predominantly across Africa in the twentieth century[4] and the presence of its bacterial agent *Yersinia pestis* in wild host populations globally. Anthropogenic climate change is predicted to increase plague prevalence across central Asia[5], with landscape modification and increased human mobility expected to further benefit the spread of plague[4].

The USA and the former Soviet Union were both interested in utilising *Y. pestis* as a biological weapon[64]. Antibiotic resistant strains of *Y. pestis*[65] and mutator phenotypes with the capability to achieve highly accelerated mutation rates[66] were isolated from wild and laboratory environments respectively. Plague therefore still poses a credible threat despite its relatively low recent activity (3,248 cases reported worldwide, including 584 fatalities in the period of 2010-2015[9]). The potential for epidemic or pandemic episodes and associated hysteria requires consistent reassessment of the growing risks associated with the ever evolving *Y. pestis* bacterium and our rapidly changing urban and rural biosphere.

Ancient DNA (aDNA) recovered from dated plague grave sites and subsequent analysis has confirmed *Y. pestis* as the bacterial agent responsible for the three major plague pandemics: the sixth century Justinian Plague[1], the fourteenth century Black Death pandemic[2] and the nineteenth and twentieth century Third Pandemic[26]. DNA recovery and sequencing techniques have improved in the past decade allowing full genome sequencing of samples from archaeological sites[19] (**Table 1**). As well as identifying *Y. pestis* as the plague's bacterial agent, this analysis has shed light on the evolutionary and geographic progression of *Y. pestis* from its source region in China[67] through three pandemic episodes, leading to its current distribution globally within the 20˚C summer

Publication	Location	Date	Sample ID	Pan/endemic
Bos et al. (2011)[19]	London (England)	1348-1350 C.E.	8124, 8291,11972	Black Death
		1350-1400 C.E.	6330	Black Death
Bos et al. (2016)[20]	Marseille (France)	1722 C.E.	"Observance"	Black Death
Spyrou et al. (2016)[68]	Barcelona (Spain)	1300-1420 C.E.	3031	Black Death
	Bolgar (Russia)	1362-1400 C.E.	2370	Black Death
	Ellwangen (Germany)	1485-1627 C.E.	549_O	Black Death
Wagner et al. (2014)[23]	Bavaria (Germany)	525 C.E.	A120, A76	Justinian
Rasmussen et al. (2015)[21]	Sope (Estonia)	2575–2349 B.C.E.	RISE00	Bronze Age
	Chociwel (Poland)	2135–1923 B.C.E	RISE139	Bronze Age
	Bulanovo (Russia)	2280–2047 B.C.E.	RISE386	Bronze Age
	Kapan (Armenia)	1048–885 B.C.E.	RISE397	Bronze Age
	Kytmanovo (Russia)	1746–1626 B.C.E	RISE505	Bronze Age
	Afanasievo Gora (Russia)	2887–2677 B.C.E.	RISE509	Bronze Age
		2909–2679 B.C.E.	RISE511	Bronze Age

Table 1. *Yersinia pestis* DNA recovered from grave sites, providing evidence of strain association with pandemic and endemic (Bronze Age) episodes.

isotherms[26]. Further historic 'Plague' episodes; the plague of Athens (430-427 B.C.E.) and the plague of Antonine (165 – 180 C.E) are now assumed to not represent true plague (*Y. pestis* infection, leading to bubonic, pneumonic or septicemic plague) with similar genetic evidence suggesting typhoid fever as the potential cause of the former[69] and either smallpox[16] or measles[70] responsible for the latter.

Y. pestis is a gram negative bacteria which diverged from MRCA, the gastrointestinal pathogen *Yersinia pseudotuberculosis,* ~53,000 years ago (95% HPD 34,659-78,803)[21] likely within the source region of the Qinghai–Tibet Plateau[22,67]. This divergence estimate and estimates determined by similar studies rely on the 'Molecular Clock' method to determine the timing of divergence events, and are implemented in palaeobiology to estimate divergence events in deep time. This method uses current genetic data from extant plague strains to determine the level of 'genetic difference'; this difference is then time calibrated, in this case using the aDNA identified through

archaeological grave site investigations (**Table 1**). Modern studies implement software (BEAST[71]), and a relaxed clock method is used, which does not assume a constant evolution rate across linages and is particularly relevant for *Y. pestis* which shows an extremely variable fixation rate[22]. This method has some limitations (as discussed by Benton et al. (2009)[72]), with early molecular clock studies predicting unexpectedly early divergence dates[73]. Methods have improved since these early studies; however divergence estimates are still best viewed in conjunction with alternate lines of evidence. In palaeobiology this requires synthesis with the fossil record to provide a minimum constraint for divergence dates. Whereas fossil evidence provides a date with relative certainty, these necessarily post-date a divergence event. In the case of plague studies (**Figure 1**), a combination of genetic, archaeological and historical evidence provides minimum constraints with varying levels of certainty.

Y. pestis' MRCA, *Y. pseudotuberculosis* is a soil/water-borne enteropathogen, transmitted via the faecal-oral route causing mild yersiniosis, which exhibits several symptoms from fever to diarrhoea[74]. Conversely, *Y. pestis* infection is severe and often fatal, with even small outbreaks capable of triggering mass hysteria, such as the 1994 Indian plague outbreak[75] which may have cost the Indian economy significantly in the ensuing years through the effect on tourism and trade[76]. Recent climate change, landscape modification and human mobility may have increased plague prevalence recently, particularly in Africa. Future climatic perturbations will probably increase plague in North America and Central Asia[4]. 3,248 cases of plague were reported worldwide across 2010-2015[9], including 584 fatalities , quantifying plague's current level of risk. Recent research suggests that climatic conditions which positively influence plague cases, namely warm springs and wet summers, may become more prevalent[4]. In 1995 a strain of *Y. pestis* was isolated from a patient in Madagascar showing bubonic plague symptoms, which showed resistance to all regularly used antibiotic treatments (chloramphenicol, streptomycin, and tetracycline, sulphonamides and tetracycline) and further alternatives used in classic therapy[77]. In 1997 a further strain was isolated once again from a human case in Madagascar with differing resistances, suggesting multiple occurrences of the newly evolved resistance traits[78].

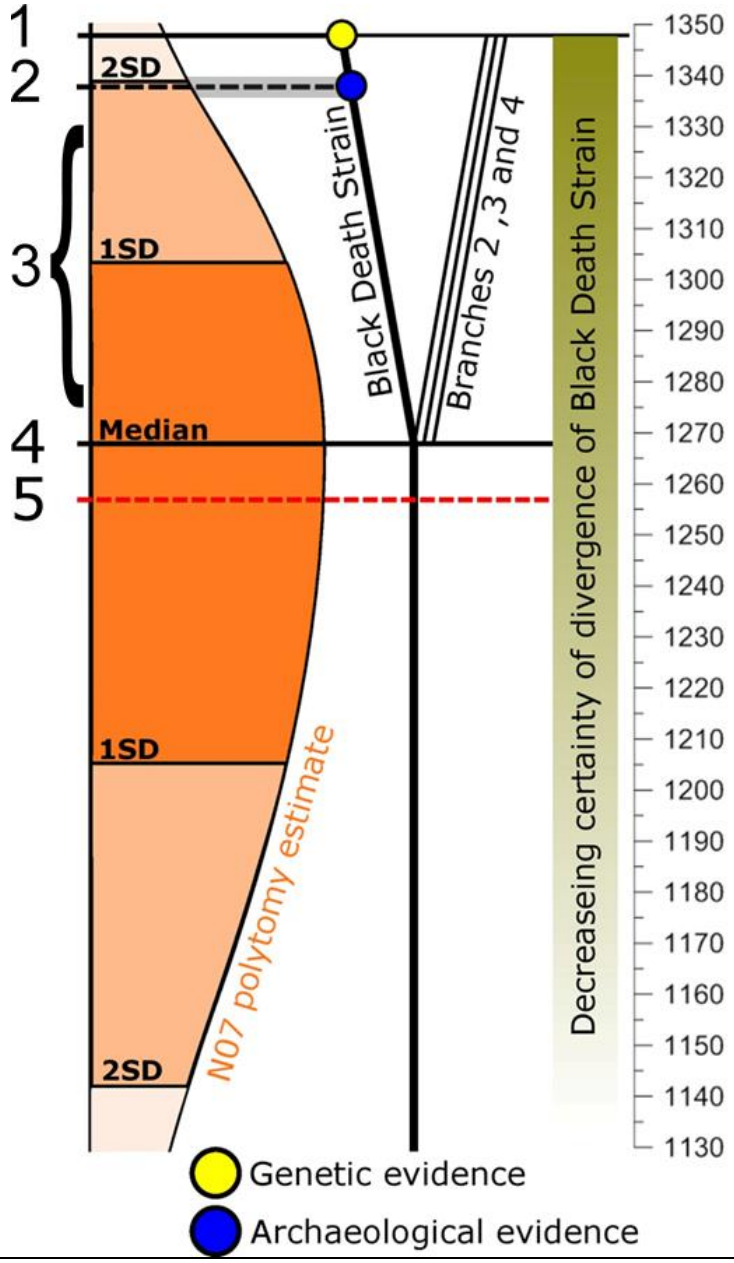

Figure 1. Synthesis of the 'Big Bang' polytomy date with further genetic, archaeological and historic evidence. The skewed normal distribution represents the polytomy estimate suggested by Cui et al. (2013)[22] with median and standard deviation values shown. The central black plot schematically illustrates the polytomy event with Branch 1, responsible for the Black Death strain and the later Third Pandemic highlighted with archaeological and genetic evidence of the divergence event shown. The gradated green plot illustrates the decreasing confidence (from dark to light) in the polytomy and thus the existence of strain branches 1-4 prior to the genetic data recovered from the East Smithfield site[19]. (**1**) Recovered DNA evidence showing the Branch 1 strain responsible for early Black Death victims; This evidence provides certainty that the previous divergence has occurred by this point, analogous to the earliest fossil evidence of a species following evolutionary divergence. (**2**) Earliest Archaeological evidence of human deaths during the Black Death pandemic from grave sites proximal to Issyk-kul[17] ;provides evidence suggesting that *Y. pestis* had caused human fatalities, however because no DNA evidence has been recovered from either site (Pishpek or Tokmak) no evidence regarding the divergence can be gleaned. (**3**) This period contains initial historical evidence of early plague outbreaks, with the weight of evidence suggesting first human infection around 1330 C.E.[18,79], however some records suggesting plague epidemics as early as 1211 C.E. however this evidence is rare and currently untestable. (**4**) Median of the polytomy estimate[22]. (**5**) 1257 C.E. Samalas eruption, the largest single volcanic forcing event of the Common Era[44].

These resistant strains of *Y. pestis* may have arisen under natural conditions in the flea midgut through plasmid transfer potentially from *Escherichia coli* (*E. coli)*[65]. Mutator phenotypes of *Y. pestis* exhibiting mutation rates of 250-fold wild type *Y. pestis* rates were discovered in archival *Y. pestis* strains stored within Georgian laboratories. The mutator phenotype may have originated through extended storage in poor conditions, and no evidence exists of its occurrence in wild populations. A naturally occurring wild *Y. pestis* mutator phenotype could aid in explaining highly irregular fixation rate of *Y. pestis* genomes through time. Further evidence acquired from current *Y. pestis* bio-surveillance projects may yet provide evidence of mutator phenotypes occurring within wild populations[66].

Pneumonic plague has the highest fatality rates of the *Y. pestis* infections[12]. Its availability and potential for large scale production and aerosol dissemination has driven global fears over its use as a biological weapon. During the Second World War Japan was reported to have dropped plague infected fleas over densely populated areas of China, following this report the USA and the former Soviet Union both began developing methods of weaponizing plague aerosols however there is no record of such a weapon subsequently being used[64].

2.2: Forms of *Yersinia pestis* infection

There are three primary forms of infection achieved by *Y. pestis* through varying pathways with differing fatality rates; pneumonic, septicemic, and bubonic plagues.

2.2.1: Pneumonic Plague

Pneumonic plague is the deadliest plague infection causing fatality rates of near 100% if untreated[12,13]. The bacterial infection induced within a victim's lungs will cause fulminant pneumonia (a severe onset inflammation of the lungs), with the symptoms ranging from coughing up discoloured mucus, struggling for breath and fever. The disease is biphasic, with initial stages showing little inflammation or symptoms whereas the final phase is highly inflammatory[13]. It is transmitted through inhalation of aerosols harbouring the bacterium, most commonly from person to person, however humans can also occasionally develop this form from one of the other modes of infection[4]. Despite its highly contagious

nature, isolating patients or utilising a thin gauze mask when in contact with infected patients have proved ample to avoid transmission[80]. Pneumonic plague is less common than bubonic plague and once identified easier to limit the spread of through isolation of patients. The human to human transmission route also requires significant human travel to transmit over large distances whereas bubonic plague can progress through a large range of wild populations and is therefore capable of spreading large distances irrespective of human transmission. However the potential for transmission over large distances has hugely increased since air travel has become commonplace. For example Severe Acute Respiratory Syndrome (SARS), which is similarly spread via aerosol droplets was spread from Hong Kong to Beijing and on to Inner Mongolia, Taipei, Bangkok, and Singapore through initial transmission on a single flight in 2003[26]. Within the evolution of *Y. pestis* early strains, upon branch 0 (**Figure 2**), demonstrate the capability of inducing pneumonic plague. An adaptation of the *pPCP1* plasmid, which occurred soon after the divergence from *Y. pseudotuberculosis*, may have facilitated the pneumonic plague transmission[12].

2.2.2: Septicemic Plague

Septicemic plague occurs when *Y. pestis* is spread through the circulatory system[9], usually following prior bubonic infection within the lymph nodes (secondary infection) however septicemic plague can also arise in patients following an infected fleabite (up to 30%) showing no buboes (primary infection)[10]. This form of plague is caused by sepsis and has a higher fatality rate than bubonic plague[11].

2.2.3: Bubonic Plague

Bubonic plague is so called due to easily identified “Buboes” forming on those infected, which are enflamed lymph nodes commonly around the groin (inguinal node) or armpit (axillary node)[7]. The bubonic form is the most common plague infection pathway and it is commonly associated with the Black Death, despite its mortality rate of 40 - 70%[4]

(66% fatality prior to the use of antibiotics and 16% with use of antibiotics[8] in modern

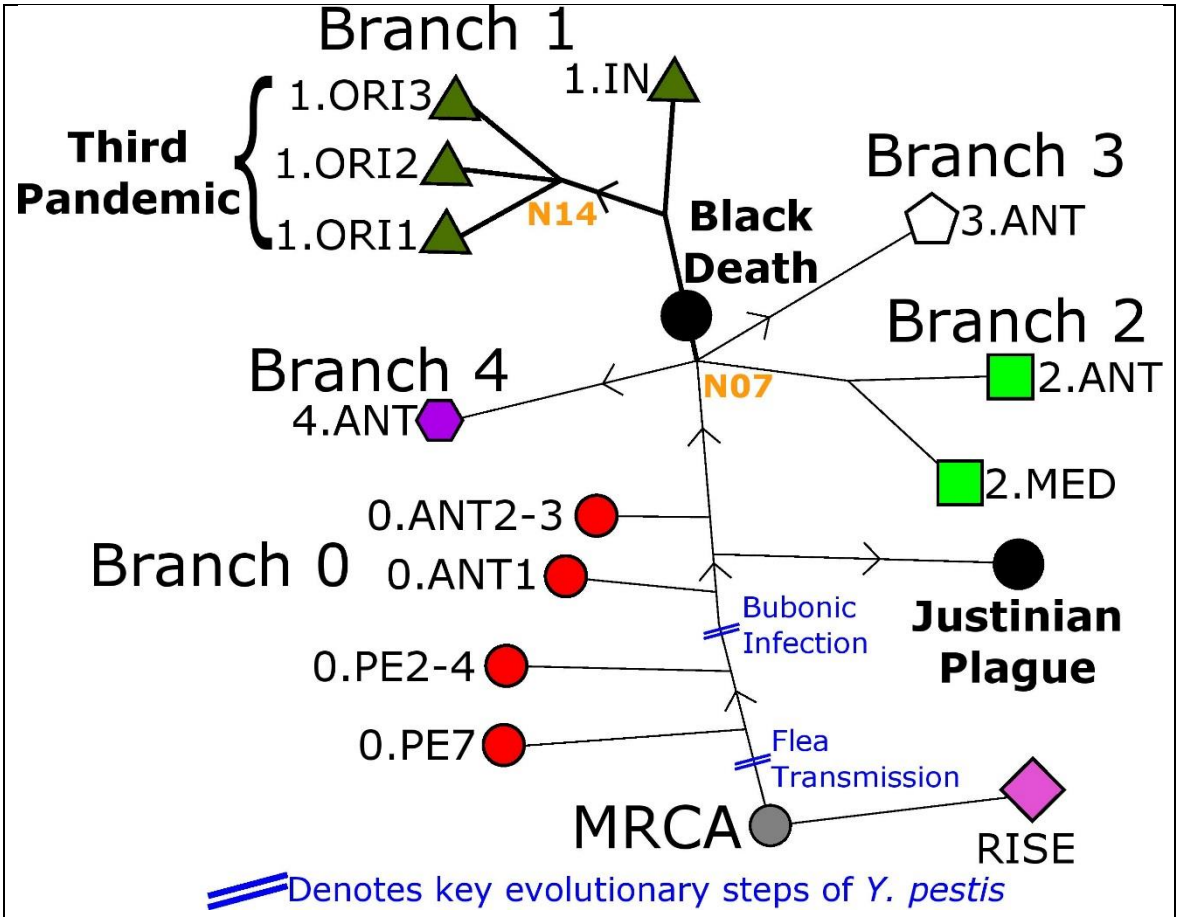

Figure 2. Simplified minimum spanning tree of *Yersinia pestis* genome (adapted from Cui et al., 2013[22]) Branches are indicated by symbols. Key evolutionary adaptations are shown: i) Flea transmission through acquisition of *ymt* gene and ii) bubonic infection facilitated by amino acid I259T substitution of the *pla* protein and loss of function in the *pde3* gene[3,12,21]. Strains responsible for specific pandemics are highlighted: i) Justinian Plague - extinct Branch 0 strain interleaved between 0.ANT1 and 0.ANT2[23], ii) Black Death strain proximal to base of Branch 1 and iii) the N07 (Orange Text) polytomy[22] and Third Pandemic strain from the current extremity of Branch 1 and succeeding the N14 (Orange Text) polytomy[22,25]. Branch 1 is further highlighted (in bold) as it contains the strains responsible for the two most recent pandemics. RISE strains(Pink Diamond) suggested to have caused brief endemic episodes prior to the acquisition of flea transmission[21].

cases from the USA), lower than both other forms of infection. Bubonic plague's infection pathway is therefore critical to its global infamy and association with all three major plague pandemics. Through the use of the molecular clock method and aDNA calibration, the final genetic change (loss of function of the *pde3* gene and amino acid I259T substitution of the *pla* protein, which enabled bubonic infection) is estimated to have occurred after 1000 B.C.E and prior to the divergence of the first branch 0 Antiqua biovar (0.ANT1), estimated at a median date of 150 B.C.E. (609BC – 205 AD 95% HPD interval)[21]. Bubonic plague is a vector (arthropod) borne disease relying on transmission of *Y. pestis* from an infected rodent or human (via the human body louse, *Pediculus humanus*[6]). The oriental rat flea *Xenopsylla cheopis* is most commonly associated with the *Y. pestis* distribution, through its association

with black rats, often considered pivotal to spread of plague within urban environments. However due to the near global distribution of plague, *Y. pestis* is now associated with a huge range of host and vector species. *Y. pestis* is relatively unique within vector borne diseases because it is confined to the vector's digestive tract and is transferred through vectors regurgitating the infected blood meal when they feed on subsequent hosts, instead of transmitted through vectors' saliva[81]. Transmission can therefore occur the first time the vector feeds after an infected blood meal or for up to a month after the infected blood meal. *Y. pestis* forms a biofilm in the proventriculus (valve between digestive tract and midgut) of the arthropod which eventually isolates *Y. pestis* to the digestive tract, aiding in regurgitative infection. *Y. pestis* isolates itself to the digestive tract through rapid multiplication which leads to the formation of a biofilm, this ability is associated to three key genetic losses (*pde2*,*rcsA* and *pde3*) following divergence from *Y. pseudotuberculosis*[82]. *Y. pestis* is non-toxic to fleas and therefore does not inhibit their ability to infect further individuals[81]. However the biofilm formation and gradual proventriculus closure leads to starvation of the arthropod, which is accompanied by repeated attempts to feed[83], thus actively increasing flea activity, and subsequently potential infection. After host infection is achieved, the infection spreads around the body via the lymphatics to the lymph nodes, leading to the formation of buboes[7]. The most commonly affected nodes are on the surface proximal to the point of bacterial entrance (flea bite) however internal nodes such as the intra-abdominal node (within the abdomen) can also contract infection and are potentially misdiagnosed as primary septicemic plague as plague symptoms are presented without the easily identified surficial buboes.

2.2.3a: Climatic controls

The initiation of a bubonic plague epidemic is reliant upon a vast array of external factors due to the necessary interaction between the bacterium, vector, host and eventually human population. Transmission is therefore influenced by a range of external factors often with further influences at a secondary stage. This creates a complex system when relating plague prevalence to external variables, such as temperature or precipitation in a particular area.

The area southeast of Lake Balkhash in Eastern Kazakhstan is inhabited by the great gerbil (*Rhombomys opimus*), a major host species of *Y. pestis* which enables plague to persist as an endemic disease in wild populations regularly varying from enzootic (effecting limited individuals in a particular area or season) to epizootic (wide spread in the host population). Vector and plague presence was recorded in detail from 1949-1996 due to the major *Y. pestis* host species in this area and the associated risk to human health. Following the discovery of plague proximal to human communities, it was dealt with through insecticides and rodent removal. Through determining estimates of occupied burrow systems and the number of gerbils and fleas (multiple *Xenopsylla* species) per burrow system, combined with burrows per hectare, flea and gerbil density estimates were produced annually. Plague prevalence was determined initially (1955-1970) through bacteriological tests, reliant on isolating *Y. pestis* from blood or flea homogenates, post-1970 serological techniques were used to identify the flea antibodies, which provided evidence of plague presence/absence in the population but not the individual[28]. These data are invaluable when studying environmental impacts of plague prevalence, particularly climatic variables, however the limited geographical range of these data requires consideration.

An early plague investigation in this area identified that epizootic episodes were triggered when host populations surpassed a threshold value for plague prevalence. Gerbil abundance (either determined by occupancy of burrow systems or gerbil density) and plague were correlated with a one to two year lag[28]. Subsequent studies identified climatic variables, specifically spring temperatures and summer precipitation, as pivotal in influencing gerbil and flea densities on an annual scale. Spring warmth is testament to early warming and because the flea vectors are only active above 10°C[30,84], a longer period of population growth increases flea density and consequently also increases plague risk. Summer humidity further correlates with flea burden (flea to host ratio), also increasing plague prevalence. Warm and wet conditions influence gerbil numbers in a similar way by increasing populations and therefore epizootic risk within the Balkhash area[29]. This amplifies the climatic impact as host and vector abundances increase in parallel under

similar climatic conditions compounding plague prevalence. The climatic correlations suggested in previous studies were then tested over millennial timescales by Kausrud et al. (2010)[5], using climatic reconstructions derived from a combination of dendrochronological records, ice core and isotope series. Investigations of climatic influences upon plague prevalence through time regularly utilize long term proxy data such as tree ring width and ice core records to estimate climatic perturbations ranging over centuries to millennia. These enable investigation and integration of historic plague pandemics with modern studies. However the proxy data provide a lower temporal resolution than recent monitoring or instrumental studies, therefore annual climatic variation was investigated as opposed to seasonal changes identified as pivotal in the Balkhash area[29,30]. The 'trophic cascade' hypothesis is often used to investigate historic plague pandemics, where an increase in primary productivity (in the case of plague studies in Central Asia, through warm and/or wet conditions) contributes to heightened plague prevalence through increasing host and vector populations. Climate-driven models of plague influenced primarily by an increase in productivity through temperature and precipitation (trophic cascade) correlate well with independent human plague records, particularly before increased local plague monitoring, antibiotic and insecticide use around 1949[5,85]. The models produced suggest peaks in sylvatic plague coincident with historic plague outbreaks. The peak model climatic conditions during the Black Death are also supported by Mongol expansions of the time which are consistent with high productivity in the Central Asian grasslands[5]. Recent and continued predicted warming may increase plague prevalence across Central Asia in the coming years[5].

Tree-ring-based climate proxies across Europe and Asia enabled Schmid et al. (2015)[33] to suggest successive reintroduction of plague into Europe following the initial 1347 C.E. Black Death introduction. They suggest that plague reintroductions were driven through preferential climatic influences on Asian host species followed by subsequent gradual progression across Eurasia. True reintroduction events were identified by utilizing a digitized database of historic plague during the Black Death[86], to determine outbreaks which were temporally (two years) and geographically (<500 km to nearby cities, and <1000

km to nearby harbours) isolated. This produced sixteen independent years of potential reintroduction. Climatic variations across Europe and Asia were then analyzed in association with the reintroduction events. No significant climatic patterns were identified across Europe associated with re-introduction events suggesting a climate sensitive reservoir within Europe was not responsible. However, the majority of reintroduction episodes showed synchrony with climatic fluctuations in central Asia[33]. The reintroduction episodes coincided with tree ring width values from juniper trees in Mongolia and the Tian Shan mountain range which suggested an increase in primary productivity and therefore potentially larger vector and host populations leading to greater plague prevalence. This was immediately followed by a decrease in primary productivity which may have forced infected vectors to find alternative host species, and consequently initiated a chain of infection culminating in plague in Europe following a lag of 15 ± 1 years due to transmission time. This hypothesis does not require a currently unidentified host species within Europe in addition to the black rat populations associated with Southern European and Mediterranean port cities. On the other hand, recent genetic investigation of skeletal remains from the Great Plague of Marseille (1720–1722), refute this hypothesis because the *Y. pestis* lineage identified is not found in extant populations and is most closely related to the strain identified in the St Mary Graces individual from London dated roughly four centuries earlier[20]. The close genetic relation between these strains suggests the presence of a permanent host species in Europe allowing the gradual in-situ mutation of *Y. pestis* as opposed to successive plague reintroduction from Asia introducing strains which differ very little despite isolated introduction events. This disagreement highlights a disparity within plague studies from differing disciplines and suggests studies of *Y. pestis* would benefit greatly from large research groups capable of providing insights from a range of disciplines.

2.3: Historic Plague Pandemics

2.3.1: Justinian Plague

The Justinian Plague, so called due to its initiation during the reign of the Byzantine/East Roman Emperor Justinian I, devastated the early medieval world causing an estimated 25 million fatalities[1]. Plague remained active into the eighth century[16],

coinciding with the cooling associated with the LALIA, and influenced social and governmental upheavals not only across Europe, but across Asia as well[43].

The Justinian Plague may have begun in Pelusium, a relatively small port city in Egypt at the eastern edge of the Nile delta. From this point *Y. pestis* then travelled a short distance west up the coast to the city of Alexandria, which at the time was the second largest city on the Mediterranean and one of the busiest ports, transporting slaves, ivory, grain paper and oil throughout the Mediterranean. This allowed rapid dissemination of *Y. pestis* in association with its host species, black rats (*Rattus rattus*) which harbour the common plague vector, the oriental rat flea (*Xenopsylla cheopis)*. Black rats were rampant across the Roman Empire at this time and after initial spread through shipping routes, plague may have spread further in association with overland grain transport and other foodstuffs likely to attract rodents. Prior to *Y. pestis* arriving in Pelusium, its movement is less certain. Plague may have spread from a source region in East Africa ("Ethiopia", the Kingdom of Aksum)[24] where it was potentially endemic for many years. The four great African port cities of the time show a decrease in ivory production coinciding with the Justinian Plague. Keys. (2000)[46] suggests that, from the period 400-540 C.E., 120 major ivory artworks are still in existence from an estimated 40,000 made, however only six remain from the period of 540-700 C.E.[1,46]. This provides limited circumstantial evidence supporting East African plague genesis prior the initial infection in Pelesium and there may have been several other explanations such as increased political instability with the establishment of the barbarian kingdoms in the Byzantine/ Eastern Roman Empire[87] which could have affected the survival of ivory goods. The East African source region is very poorly defined, and requires further evidence, however the potential for *Y. pestis* transport from East Africa to its Mediterranean initiation is often considered[1,24].

Progression of *Y. pestis* from the potential East African source to the Mediterranean may have required climatic cooling, potentially caused by volcanism[24], to allow transmission of host, vector and bacterium up the Nile through the heat of the Sahara. However further work is required to provide supporting evidence, with a recent genetic investigation suggesting the Justinian Plague *Y. pestis* strain had its source within central Asia[23]. This

further complicates the story as *Y. pestis* transmission from central Asia to the Mediterranean via Africa requires previous transmission from central Asia, most likely to India then on to Africa through potential Sea trade[24]. Irrespective of the initial route of transmission the combination of the severe plague death toll, and the inhibited agriculture due to the LALIA, contributed to global upheaval in the ensuing centuries with regular conflict and the rise and fall of several Eurasian Empires[43].

2.3.2: The Black Death

2.3.2a: Transmission from source to Europe

The Black Death is the most infamous pandemic episode and caused reduction in populations in Europe of between 10-60%[88] (Dennis et al. (1999)[7] suggest that fatalities across Eurasia and Africa totalled 50 million) with further estimates equating fatalities to roughly one third of the global population[89]. Nestorian grave sites from the small settlements of Tokmak (now Tokmok) and Pishpek (now Bishkek), both proximal to Issyk-kul (Kyrgyzstan)[17], provide the first evidence of Black Death fatalities. From this point *Y. pestis* travelled westward along the 'Silk Road' in association with grain and fabric transport and the rodents they often unwittingly transported. Mongol caravans, soldiers and riders regularly in transit across the Asian Steppe would have also aided in *Y. pestis* dissemination[18]. Plague reached the Genoese port city Kaffa (on the coast of the Black Sea), in 1346 C.E. while it was being besieged by Khan Janibeg's Mongol army[3]. Gabriel de Mussis a lawyer of Piacenza and a major source documenting plagues arrival in Europe[90] writes of the 1346 C.E. Mongol siege of Kaffa. He writes of Mongols launching the plague victim's corpses over the walls leading to plague infection in the city. This account was possibly falsified due to de Mussis potentially benefiting from portraying the Christian inhabitants of Kaffa having plague rained down upon them by barbaric Mongols[18]. *Y. pestis* was more likely spread through introducing infected rats to the city, however there is potential for vectors to spread *Y. pestis* to local rodent populations from a catapulted corpse. After Kaffa's initial infection, *Y. pestis* then spread rapidly throughout Europe via heavy maritime traffic on the Black Sea and the Mediterranean. Sicily was central to European trading at the time, and the arrival of plague in October 1347 C.E.[91] enabled plague to

spread rapidly around the Mediterranean. By 1348 C.E. the majority of Italy, coastal France and Spain harboured *Y. pestis*, and almost all Europe was influenced by infection by 1350[3].

2.3.2b: Mongol influence on plague

The Mongol empire expanded in the thirteenth century to its furthest reaches, stretching from the Pacific Ocean in Eastern China to Eastern Europe in the west[92]. The Mongol expansion began under the rule of Chinggis Kahn (1206-1227 C.E.[93]), potentially coinciding with an increase in precipitation across Central Asia, due to early initiation of the LIA across Asia[94]. Expansion of the empire continued following Chinggis' death in 1227 C.E. as the Mongol empire was led by successive members of the Chinggisid family with regular infighting until Kublai Khan's death in 1294 C.E. after which the empire fractured into separate Khanates.[79]

Historical accounts of plague initiation predominantly suggest the early to mid-fourteenth century as the first period of notable human fatalities across Central Asia and China[18,95]. This may have followed increased warfare and persecution within the zoonosis area suffered by Nestorian communities proximal to Issyk-kul, who provide the first archaeological evidence suggesting human plague fatalities[17]. The area south of Lake Balkhash (encompassing Issyk-kul) was established as pasture in 1250 C.E. However this was short lived, because by the mid-fourteenth century warfare had drastically deteriorated agricultural lands[79]. Some military campaigns were driven by unrest between the Khanates, such as the brief 1315 C.E. conflict, when the Yuan Khanate (Eastern) moved deep into Chaghadaid territory (Central), reaching their winter pastures near Issyk-kul where Yuan soldiers are reported to have "looted their wives and children"[96]. At a similar time, Christian persecution through gradual Islamization across central Asia further damaged the Nestorian communities placing them in a highly fragile state, potentially more susceptible to infection through general ill health and malnourishment[42].

An early reference of plague spreading in Central Asia occurs in the accounts of Ib Al-Wardi, an Arab scholar. He suggests that "The disease began in the land of darkness" (interpreted as Mongolia or Inner Asia[95]) and that "pestilence raged in the east for fifteen years before arriving in the West", which suggests a start date around 1331 C.E.[18]. This

closely coincides with references pertaining to: torrential rain and drought in China[18], deaths of many Mongol soldiers, princes and most notably "the premature death of the Great Kahn Jijaghatu Toq-Temur" and his sons in 1331/1332 C.E.[18,95] as well as a mystery illness in Hopei province devastating the population in 1332 C.E.[18]

2.3.2c: Preconditioned European populations

Significant agricultural damage occurred across Europe prior to the *Y. pestis'* introduction. 'Plagues' decimated domestic sheep (via 'Sheep Scab' decimating British flocks in 1279 C.E.) and cattle (via 'The Great Bovine Pestilence' of 1319-1320 C.E., whose likely culprit is rinderpest) populations in the preceding half century. The latter epidemic followed closely after persistent terrible yearly harvests particularly across England due to prolonged torrential rains, which contributed to the Great Famine (1315-17 C.E.). Famine and nutritional deficit caused by respective shortages of grain (contributing to 70-80% of daily caloric intake) and dairy products (10-15% caloric intake) would have damaged populations across all demographics but may have caused particularly intense food shortages in subsistence farming areas. However, little bias is observed in plague burials towards individuals with tell-tale skeletal stress markers[97] which is symptomatic of survival through famine. This suggests either that surviving the Great Famine did not predispose populations to higher plague prevalence, or that *Y. pestis* had a homogeneous influence irrespective of prevailing health conditions.

2.3.2d: Recent genetic advances

Further to historic evidence estimating the initial timing and location of the Black Death pandemic, recent scientific studies have produced independent results employing identified *Y. pestis* strains, both extant in current host species reservoirs and identified through aDNA investigation. Cui et al. (2013)[22] utilised georeferenced strain data from across Asia and the genetic information recovered from the East Smithfield Black Death Cemetery (historically dated to 1348-1350 C.E.[19]) to map the evolutionary pathway of *Y. pestis* associated with the two most recent plague pandemics. An area encompassing the Western Qinghai-Tibetan Plateau was suggested as the source region for *Y. pestis* following its divergence from *Y. pseudotuberculosis;* this was due to the earliest strain

identified at the time (0.PE7) isolated solely in this area. Recent research has identified earlier *Y. pestis* strains that were active across Eurasia[21], however 0.PE7 remains the earliest identified strain capable of effective flea transmission. This geographically confined area encompassed the most diverse strain isolates across Asia, further supporting Cui et al's (2013)[22] conclusion that this was indeed the source region. Genetic comparative analysis further revealed two previously undocumented branches, 3 and 4 (**Figure 2**), which diverged from the ancestral branch 0 at the same time as branch 1 and 2. This divergence node (N07) represents a polytomy event (a point when greater than two branches appear to diverge simultaneously) commonly termed the 'Big Bang'. A further polytomy (N14) was identified at the base of the 1.ORI strain group, which was responsible for the Third Pandemic and now shows the largest geographic range across all continents except Antarctica[25]. The molecular clock method was used to determine estimated dates of these polytomies with median dates for N07 and N14 respectively of 1268 C.E. (1142-1139, 95% Cl) and 1808 C.E. (1735-1863 C.E., 95% Cl). As expected, these estimates both predate the first human infection identified within the pandemic episodes, with Cui et al. (2013)[22] suggesting these bursts in diversification are due to greater replication cycles during epidemic periods when compared to enzootic periods. However, climatic factors positively influencing host density could also have driven the rapid diversification observed. A subsequent study focusing on divergence of pre-Bubonic 'RISE' strains of *Y. pestis,* suggests an earlier divergence date for the strain responsible for the Black Death pandemic, 1160 C.E. (901-1343 C.E. 95% HPD) however the previous N07 estimate,1268 C.E. is well within the 95% highest posterior density estimate. Through synthesis of aDNA identified from the Justinian pandemic, Wagner et al, (2014)[23] suggest that due to extensive rate variation in *Y. pestis* evolution, use of molecular-clock derived divergence estimates are likely erroneous. This highlights the need for further work in this area which would benefit from further aDNA evidence from varying stages in *Y. pestis* evolution.

Hymes (2016)[98] attempted to reconcile the estimated 1268 C.E polytomy date with historical evidence from the early Chinggsid (Mongol) expansion. The Mongol conquest of Xia (a historical region now encompassing Gansu) is discussed due to its proximity to Cui

et al.'s (2013)[22] suggested source region, as well as lying within the range of the Himalayan marmot, a known *Y. pestis* host species. The Mongol campaign against Xia lasted from 1205-1227 C.E. with tangential references to 'pestilence' or 'epidemics' surrounding Mongol warfare from 1211-1273 C.E. These references however provide little certainty as to the nature of the disease described and are therefore insubstantial as proof of early epidemic plague outbreaks.

2.3.2e: Longevity and impact

Plague conditions associated with the Black Death persisted within Europe with significant impetus until the seventeenth century with occasional isolated cases occurring into the nineteenth century prior to the initiation of the Third Pandemic[86]. Further to the devastatingly rapid population decrease across Europe, economic prosperity was greatly influenced. Real Gross Domestic Product (GDP) across Europe was instantly damaged by the Black Death whatever economic conditions prevailed prior to the Black Death, with Spain, Italy and England all showing real GDP decrease by 15-35% below immediate pre-plague levels and persisting as late as 1500 C.E.[3]. European plague initiation was closely followed by adverse climatic conditions particular across England and Italy damaging arable and pastoral production with particular severity in 1348/9 C.E.

Other industries were damaged as well, with lead mining in England coming to a complete halt at the initiation of the pandemic (1349-53 C.E.), leading to the lowest lead (Pb) concentrations identified in an Alpine ice core[99]. Agricultural land decreased in value predominantly through an increase in availability because of a collapse in demand due to population decreases as well as an initially limited workforce to tend the land. Land price exerts significant influence on national and regional economies, and therefore helps to explain the severe and sustained drop in GDP[3].

Outside of Europe similar influences of the Black Death pandemic were observed; for example Egypt suffered rapid depopulation within the Nile delta, leaving "No one left to gather the crops" (Borsch, 2016)[100], with plague reaching its peak in Cairo in 1348 where an estimated 7,000 people perished per day[2,100]. Plague further influenced significant swathes of Asia including the Arabian Peninsula and persisted in Ottoman areas and also

Western Europe until the mid-nineteenth century. Studies of plague prevalence and persistence both historically and scientifically are however much rarer beyond the reaches of Europe. This highlights the Eurocentric bias within plague studies, with the majority of historic evidence derived from contemporary European accounts, and even recent aDNA studies showing a bias towards European grave sites pertaining to the first two major plague pandemics[2,101].

2.3.3: The Third Pandemic

The so-called 'Third Pandemic' had the largest geographic range, however it caused the lowest number of fatalities, estimated at around fifteen million[14] predominantly in Asia. Plague epidemics in human populations associated with the Third Pandemic initiated in Yunnan Province in the 1850-60s[15], and spread gradually across China until reaching the port cities and trading hubs, Guangzhou (formerly Canton) and Hong Kong in 1894 C.E.[102]. This crucial step in the *Y. pestis* transit allowed plague to spread through the international shipping routes, often aboard steam ships of the British Empire[14], and establish foci in suitable populations within the Northern and Southern 20°C summer isotherms[26]. Despite this global expansion, plague caused limited fatalities outside Asia although plague host populations increased globally until the mid-twentieth century[14].

The Mohammedan Rebellion within the Gansu region of China, a region with significant himalayan marmot populations, a known host population, may have contributed to initial human infection in the 1850s[15]. This period also coincides with the Panthay rebellion in Yunnan province which began in 1856 C.E. when Qing officials initiated a massacre of the regions Muslim population (Hui) lasting three days, with subsequent and extremely violent episodes continuing until a final massacre with an estimated ten thousand fatalities in Dali City in 1873 C.E.[103]. This shows similarities to the Black Death where the first victims of *Y. pestis* were also within areas of warfare and suppression, further suffering due to prolonged and limited agricultural yields[104], no doubt contributing to substantial ill health and famine in the region. The systematic link between impoverished and malnourished populations and plague is very general, with human immunizing agents restrained through nutrient deficiencies[42]. Malnutrition could therefore have contributed to

the dissemination of disease through these populations; however the association of *Y. pestis* with these particular groups suggests that exposure to a particularly susceptible population is pivotal to pandemic plague initiation and spread. Increasing food scarcity in the coming years due to continued population growth, water shortages and migrating climate belts[105] in combination with climatically preferential conditions for *Y. pestis*[4] suggests that this is an area that warrants extensive further research.

Y. pestis' spread globally following its arrival in South Western Chinese port cities and introduced plague to three continents that had never experienced it before. The Orientalis (1.ORI) strain responsible for the Third Pandemic is thought have evolved in or proximal to Yunnan province and its subsequent spread means this strain has now established near global distribution[25] and is therefore responsible for all cases within North America, South America and Australia. Densely populated areas within China and India contained the majority of global fatalities with several British and French colonies suffering reoccurring and severe epidemics[14]. The western world generally suffered very few fatalities (**Supplementary Table 1**), with Africa recording >200,000 cases in the period of 1877-2007 C.E. following a repeated increase in prevalence peaking in 1997 C.E.[106]. Further to this continental skew in fatalities certain demographics within infected areas were disproportionately affected. Overcrowded areas regularly inhabited by a recently settled immigrant population driven by industrialization and world trade expansion, were disproportionately influenced by plague due to proximity to infected rodents and general ill health leaving people more susceptible to infectious disease. These demographically isolated groups were often subjected to harsh and culturally abhorrent measures, with these responses contributing to the 1900 C.E. Great Honolulu China Town Fire in Hawaii, initial steps towards apartheid in South Africa, and anti-Asian prejudice in the USA and Australia[14].

The progressive plague transmission through Asia culminating in the outbreak in Hong Kong in 1894 C.E. provided impetus for the scientific community to intensely study plague, with Alexandre Yersin and Kitasato Shibasaburō independently isolating the plague bacillus around the time plague reached Hong Kong. This was quickly followed by work suggesting that the disease showed a strong association with rat populations, however this

work was not generally accepted by the medical community with human transmission preferred as the method of disease proliferation, with vaccines seldom used throughout the pandemic[14].

Despite a reasonably well-documented history, no consensus exists regarding the conditions which ultimately triggered evolutionary changes in *Y. pestis* and the development of plague pandemics. This gap in our knowledge greatly limits our ability to model the advent and spread of potential future pandemics, an issue which is particularly relevant given the evolutionary progress of the *Y. pestis* bacteria towards antibiotic resistant strains and the increasing likelihood of climatic conditions positively influencing host and vector populations in the coming years.

Chapter 3: Methods

3.1: Genomic reconstruction

The minimum spanning tree of *Yersinia pestis* genomes presented by Cui et al. (2013)[22] was simplified to present key evolutionary steps and divergences (N07 and N14), with strains responsible for the three pandemic episodes highlighted. Branch points were minimised through grouping of clades. Ancient DNA providing evidence of the extinct strain responsible for the Justinian plague was added, interleaved between two extant groups, 0.ANT1 and 0.ANT2[23]. Genetic losses and gains of the *Y. pestis* genome which contributed to key evolutionary steps were added, as were the recently identified strains responsible for early Eurasian endemic outbreaks (RISE)[21].

3.2: Area selection

Selection of areas of interest was crucial to climatic and radiative reconstructions. Two areas were selected within differing climatic regimes to illustrate any variation in response to volcanic forcing events across regions potentially influential in the initiation of the Black Death plague pandemic. The **source** area (90-110°E, 30-40°N) was selected based on the suggested source area presented by Cui et al. (2013)[22] with the earliest flea transmissible strain (0.PE7) central to this area[21,67]. This area also encompasses a large section of the Silk Road which is thought to have aided in distribution of plague strains throughout Asia[25]. The source area straddles the current Asian summer monsoon limit[107] with the climate in this area therefore predominantly driven by the Asian monsoon system. The minimum size of area selected for temperature reconstruction provides 65 gridded temperature estimates with a suitably small standard error (maximum of 0.8) recorded across the mean temperature values within the periods of investigation (**Supplementary Table 1**). The **zoonosis** area (64-86°E,38-48°N) encompasses Issyk-kul and the proximal grave sites of Pishpek (Bishkek) and Tokmak (Tokmok) which show the earliest evidence of plague fatalities in human populations during the Black Death pandemic[17]. The area further encompasses the Lake Balkhash region of Kazakhstan, a source of major plague and climate studies through use of the Pre-Balkhash great gerbil (*Rhombomys opimus)* dataset recording population densities of the host and vector species as well as the local prevalence of plague[5]. The estimated route of the Silk Road runs east to west across the

area. The location to the north of monsoon limit places this area in arid Central Asia (ACA), whose climate systems are influenced predominantly by westerlies and should therefore aid in illustrating any difference in climatic response to large explosive tropical eruptions.

3.3: Atmospheric data sources and acquisition

UV-B data from NASA's Ozone Monitoring Instrument (OMI) was used to determine response in UV-B[108] radiation following the October 2010 Merapi eruption. The OMI uses hyperspectral imaging in a push-broom mode to observe solar backscatter radiation in the visible and ultraviolet[109]. OMI is mounted on the NASA Aura spacecraft which was launched in July 2004 with UV daily dose data recorded from October of the same year. Aura is in a sun-synchronous orbit at an altitude of 705 km. Data were collected continually at a daily resolution with erythemally weighted daily dose collected at a spatial resolution of 1.0° x 1.0° globally.

Data were acquired using NASA's Giovanni online environment (https://giovanni.gsfc.nasa.gov/giovanni/#service=TmAvMp&starttime=&endtime=&variableFacets=dataFieldMeasurement%3AErythemal%20UV%3B). Monthly time averaged maps of Erythemal Daily Dose (Local Noon) (Jm^{-2}) were produced for each month of operation, from the start date, October 2004, to January 2017 with data downloaded in NetCDF format. Maximum, mean and median values were then extracted for each month using R[110] with the ncdf4 package[111] and the script provided (**Supplementary Script 1**). Z-scores were further calculated for all maximum monthly UV-B values. The plot of global annual mean UV-B (Jm^{-2} day^{-1}) (**Figure 4b**) was produced by Beckmann et al, (2014)[53] and is free to access via the Helmholtz Centre for Environmental Research http://www.ufz.de/gluv/index.php?en=32435.

To create **Figure 4c**, the data values at 1.0 x 1.0 degrees were extracted for the maximum UV-B month in each year using the script provided (**Supplementary Script 1**) (excluding 2004 and 2017 due to maximum exposure occurring in summer months of June or July) with z-scores calculated by grid point for July 2011. The data produced was then plotted using contouring software (Surfer14® from Golden Software, LLC (www.goldensoftware.com)) and overlain on GTOPO 30 digital elevation map[112].

3.4: Time period selection

The zoonosis event must necessarily predate all evidence of human infection within each pandemic episode. In the case of the Black Death the zoonosis event must have occurred previous to the confirmed *Y. pestis* grave site of Issyk-kul (1338 C.E.) and the majority of reliable historical evidence (~1330 C.E.), and postdate the 'Big Bang' event which produced the *Y. pestis* strain responsible (1268 C.E., 95% CI 1142-1339 C.E.) (illustrated in **Figure 2**). This produces a potential zoonosis window of between 1268–1330 C.E. with the lower value reliant on the polytomy estimate which has a broad 95% confidence level. Climatic reconstructions will therefore focus on this time interval to determine if optimal climatic conditions could have catalysed the Black Death pandemic by encouraging zoonosis.

3.5: Temperature and volcanic forcing reconstructions

Two summer temperature reconstruction datasets were utilised across the study area (PAGES Asia 2k[61] and N-TREND[63]) to initially verify temperature response to the volcanic forcing episodes with an eleven year weighted average produced for both. An estimate of the temperature response's spatial heterogeneity was then determined using only the PAGES Asia 2k data due to its higher spatial resolution. **PAGES Asia 2k** utilises a network of annual tree ring chronologies covering the period from the ninth to the late twentieth century providing a summer (JJA) temperature reconstruction. The reconstruction covers most of continental Asia (60-150°E, 10°S-54°N), with 773 grid points at a resolution of 2.0° x 2.0°, however the temperature reconstruction is only valid form 23°N northwards. Z-scores with respect to 1750-1950 C.E. were calculated to allow direct comparison to the Eastern Eurasian N-TREND data. **N-TREND** provides summer Northern Hemisphere (NH) temperature reconstructions from 918-2004 C.E. covering the region from 40-57°N globally, utilising 54 previously published tree ring records. Wilson et al. (2016)[63] subdivided their temperature reconstructions into four NH regions with the Eastern Eurasia region (extending from 80-150°E) utilised for this study. Both temperature reconstructions were further plotted against the global volcanic forcing data produced by Sigl et al. (2015)[44]. This data provides a 2500 year revised record of global volcanic forcing derived from ice core

sulphur records from Greenland and Antarctica. The data are categorized by eruption location with divisions of NH, SH and tropical eruptions.

The high resolution PAGES Asia 2k dataset was subdivided to represent temperature reconstructions across the source and zoonosis areas. To determine an estimate of actual temperature values in each area the '0' values of the reconstructions were calculated using the calibration data applied by Cook et al. (2013)[61] in the construction of the PAGES Asia 2k dataset. The instrumental temperature field used for calibration and validation was the Climatic Research Unit (CRU) Time-Series (TS) Version 3.10 of High Resolution Gridded Data of Month-by-month Variation in Climate (Jan. 1901 - Dec. 2009) (CRU TS3.10)[113] with the years 1951 – 1989 C.E. used for calibration due to sufficient instrumental coverage during this period. The data are free to access through the Centre for Environmental Data Analysis (CEDA) and script was written to extract mean summer temp (JJA) for the source (90-110°E, 30-40°N) and zoonosis (64-86°E, 38-48°N) areas for the period of 1951-1989 (**Supplementary Script 2** written in bash (Unix shell).

Years of maximum annual post-volcanism cooling and subsequent peak warming/recovery were contoured in Surfer14® from Golden Software, LLC (www.goldensoftware.com) to determine spatial heterogeneity of the temperature reconstructions. This process was repeated to produce contoured Palmer Drought Severity Index (PDSI) plots representative of changes to hydro-climatic systems around the years of peak warming (1318-19 C.E.) and the Issyk-Kul grave date (1338 C.E.). The source data used was the Monsoon Asia Drought Atlas (MADA) produced by Cook et al. (2010)[62].

Chapter 4: Contribution of volcanism to the initiation of plague pandemics

4.1: Introduction

Yersinia pestis was responsible for millions of fatalities globally through three major plague pandemics of the Common Era[114], which persisted for centuries following their initiation with repeated localized epidemics regularly flaring. Of the pandemic events, the Black Death pandemic was the largest, killing a third of the estimated global population[89] and persisting from the fourteenth to the seventeenth century (Common Era) in Europe[115], imparting significant long term societal impact upon affected regions[116]. However, Like the Black Death, the Plague of Justinian is thought to have contributed to wider developments in European history. Rosen (2010)[1] argued that heterogeneous recovery across Europe benefited Northern and Central Europe over the previous economic centre around the Mediterranean. The so-called 'Third Pandemic' in the mid-nineteenth century enabled *Y. pestis* to be disseminated through international trading routes and establish plague foci globally[26]. This pandemic episode began in Yunnan province in the 1850s[15] and spread gradually eastwards across China until it reached the port cities of Guangzhou (formerly Canton) and Hong Kong in 1894 C.E.[102]. *Y. pestis* then spread globally through maritime trade routes at a rapid pace due to recent improvements in the speed and efficiency of steamships. This allowed establishment of multiple plague foci globally in regions between the 20°C summer isotherms of the Northern and Southern Hemisphere[117] and caused estimated global deaths of around fifteen million people[14].

Climate may catalyse disease outbreaks, including plague[31,33] .Climatic variation influences *Y. pestis* prevalence through interactions with host and vector populations[30]. Studies of established plague foci have determined particular climatic conditions beneficial to the spread of *Y. pestis* which persisted preceding pandemic episodes[29]. Increased primary productivity regularly shows positive correlation with host rodent populations and vector density, which consequently increases the potential for human infection[5]. Studies integrating host rodent (great gerbil, *Rhombomys opimus*) and vector (fleas mostly in the genus *Xenopsylla*) data collected from the Balkhash area of Kazakhstan, with regional climatic data, suggest certain climatic factors positively influence plague prevalence. Warm

springs and wet summers positively influence host and vector populations, which following a lag of one to two years positively influences plague prevalence both within rodents and subsequently local human populations[29,30]. Due to the resolution of climatic proxy data it is often not feasible to consistently reconstruct monthly to seasonal variations therefore studies attempting to determine the influence of climatic variables relating to any of the three major plague pandemics often apply the 'trophic cascade' hypothesis. The 'trophic cascade' hypothesis is generally applicable to plague, with conditions that increase primary productivity such as increased temperature and, particularly in relation to the wealth of plague reservoirs within arid Central Asia, precipitation positively influencing plague associated species and coinciding with epidemic and pandemic episodes[5,32,33]. Extreme weather events, such as flooding and heat waves, can promote contact between rodent and human populations depending on the environmental norms in an area, leading to an increased probability of zoonosis[118]; in fact the initiation of all three plague pandemics coincide with exceptional rainfall[23]. The first archaeological evidence of the Black Death is a grave site in Issyk-Kul (Kyrgyzstan) where an inscription detailing a fatality due to plague dated to 1338 C.E. has been identified and the annual burials substantially increase[17]. This event coincides with initial Himalayan and European glacial expansion symptomatic of the end of the Medieval Climatic Anomaly (MCA) and the initiation of the globally cooler period of the LIA[119].

Y. pestis was endemic (small and localized) in isolated areas across Eurasia at early stages of its evolution (2815-1626 B.C.E.) however is not thought to have caused large scale epidemics due to the much less pathogenic nature of these early strains, which were not capable of flea borne transmission. Molecular clock calculations suggest that vector transmission was not possible until 1000 B.C.E.-0 C.E. with aDNA data from Justinian Plague victims showing the first dated genetic evidence of this trait[21,23]. Although *Y. pestis* was capable of causing pneumonic plague prior to the acquisition of flea transmission, all major identified pandemic episodes occurred following flea transmission capability[12]. *Y. pestis* vectors are often transportable over large distances. In the case of the Black Death, caravans along the Silk Road[18] (**Figure 3**) may have allowed rapid distribution of an infected

flea population across a wide geographic region through movement of products such as cloth or through incremental infection of rodent populations. Gene fixation rates are highly variable within *Y. pestis,* and apparent 'polytomies' precede two of three major plague pandemics; Cui et al. (2013)[22] dated the polytomy preceding the Black Death (N07) to 1268 C.E. (median date) (**Figure 1**) and termed this the 'Big Bang' because it resulted in the development of strain branches 1-4 (**Figure 2**). Cui et al. (2013)[22] also identify the Qinghai-Tibetan Plateau as the source region of *Y. pestis* through the presence of the basal 0.PE7 strain, and recent studies suggest earlier strains caused endemic episodes in other locations across Eurasia (RISE) however 0.PE7 is the earliest strain capable of flea transmission[21]. Cui et al further state that this region is where the 'Big Bang' occurred as it contains the highest density of georeferenced *Y. pestis* strain isolates from three out of four diverged branches. They suggest that the 'Big Bang' event was caused by host demographic changes during an epidemic phase; however climatic changes could also drive host density changes, offering an intriguing alternate hypothesis. If climate mediated epizootics[60], the polytomy date should coincide with ideal climatic conditions. However, our results indicate that such conditions occurred significantly after the diversification estimate, and that the polytomy instead closely coincided with a prolonged period of increased global volcanic forcing (GVF) within which the largest single sulphate injection of the Common Era occurred, the 1257 C.E. Samalas eruption. There is a further polytomy and increase in fixation rate dated to 1808 C.E., identified at the root of the 1.ORI population, responsible for the Third Pandemic[25]. Both these polytomy dates occur within less than eleven years of two of the largest volcanic eruptions of the Common Era and within periods of prolonged elevated GVF.

The Tibetan Plateau is the second most UV-B irradiated area of the planet (only surpassed by areas of the Andes due to their lower latitude) (**Figure 3b**) with annual maxima occurring during summer months (June/July)[53]. High UV-B exposure leads to DNA damage, such as skin cancer in humans[120], genome instability in plants[121], mutagenesis in bacterial species such as *E. coli*[122], and intervals of particularly high incident rates may have contributed to rapid evolutionary bursts evident within the palaeontological record[54,55]. Some

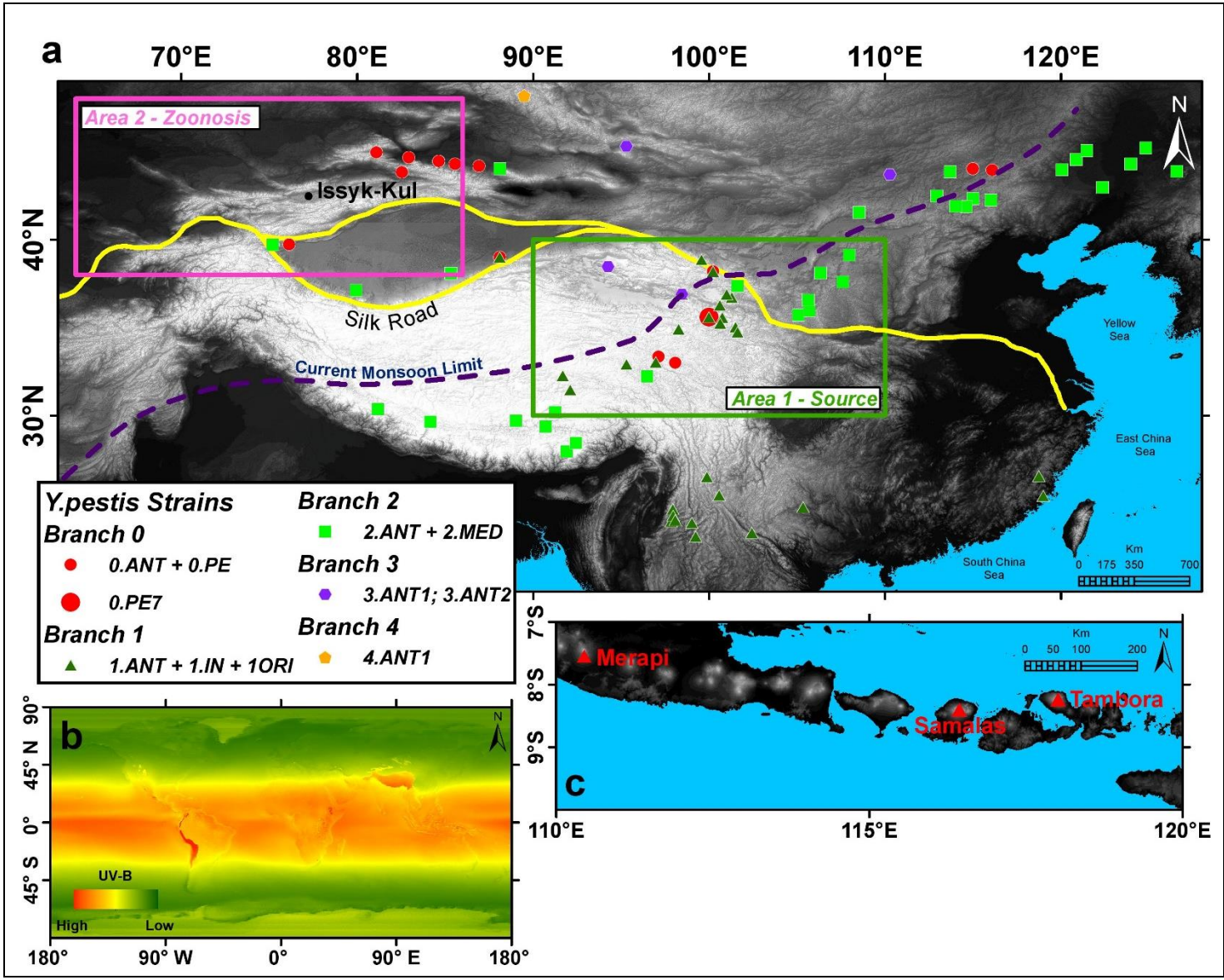

Figure 3. Historical and ecological regions of interest for *Y. pestis*. (**a**) Digital Elevation Map (DEM) of East Asia[112] showing two hypothesised areas of interest (Area 1 Source; Area 2 Zoonosis). Area 2 is based upon Cui et al.'s (2013)[22] DNA derived source region and therefore encompasses the potential source region of flea transmissible strains of *Y. pestis* (0.PE7)[67] and the highest diversity of *Y. pestis* isolates[22]. Area 2 encompasses the site of first archaeological evidence of fatalities during the Black Death pandemic identified through grave inscriptions from Issyk-kul[17,79] and the primary trade route to Europe, the Silk Road[123,124]. The symbols represent georeferenced *Y. pestis* strains identified by branch, isolated either from host populations or patients, utilised by Cui et al. (2013)[22] (**b**) Global annual mean UV-B illustrating the high UV-B values associated with high altitude areas of the Andes and the Tibetan Plateau[53]. (**c**) DEM[112] of Indonesia illustrating location of Samalas, Tambora and Merapi volcanoes.

UV-B radiation is absorbed by atmospheric ozone which effectively regulates terrestrial UV-B exposure[52] . The summer months with the highest UV-B fluxes coincide with times of activity (non-hibernation) for *Y. pestis* hosts and vector populations, such as the Himalayan marmots[125].

A link between large scale explosive volcanism and ozone depletion is well-established[48,126-129]. For example, the 1991 Pinatubo eruption reduced ozone concentrations by an estimated 2% within the tropics and 7% at mid latitudes[130]. Stratospheric ozone regulates terrestrial UV-B insolation through the absorption of incident radiation[52], with a 1% decrease in ozone resulting in 1% increase in erythemal UV-B exposure at 45° latitude[131]. A three-year period of enhanced UV-B was recorded globally following the Pinatubo eruption[132], and specifically ozone depletion contributed to a 25% increase in the 305nm irradiance. Aerosol pollution and cloud cover also influence terrestrial UV-B through scattering of incident radiation, however following large explosive volcanic eruptions UV-B values are modulated predominantly by ozone depletion rather than increased scattering[50].

Volcanic sulphur dioxide (SO_2) and halogen (e.g., chlorine and bromine) aerosol injections into the stratosphere drive ozone depletion[48]. Sulphate aerosols provide a greater surface for heterogeneous chemical reactions that enable halogen species to destroy ozone (O_3)[49,133-135]. Chlorine and bromine halogen species actively deplete the ozone; bromine is more effective by an order of magnitude, but bromine is much less concentrated in volcanic material[136]. The 1991 Pinatubo eruption produced significant levels of sulphur dioxide (20 Tg) but produced much lower levels of chlorine (3 Tg)[137]. The primary source of stratospheric chlorine at the time was therefore determined as anthropogenic[50]. Previous studies suggest that erupted halogens are entirely scavenged by hydrometeors (e.g., rain and ice) and seldom reach above the tropopause, which renders them ineffective as a catalyst for ozone depletion and instead potentially contribute to increased ozone through other processes[51,128]. The timing of the Pinatubo eruption was coincident with a tropical cyclone[138], which chemically portioned the water soluble halogen species leading to a

minimal stratospheric input of halogens[128]. Several recent studies[127] and satellite observations[139] have however suggested that hydrometeor scavenging may not beas effective in fractionating halogens, and significant levels of hydrogen halides (predominantly HCl) may be co-injected with sulphur dioxide to stratospheric altitude. Klobas et al. (2017) modelled ozone depletion following the Pinatubo eruption in a contemporary (high anthropogenic chlorine) and future (low anthropogenic chlorine) situations, with the results suggesting significant global ozone depletion even at low anthropogenic chlorine levels. This further suggests that pre-industrial eruptions had significant negative effects on the ozone concentrations, as previously suggested for the Minoan eruption of Thera (Santorini) [140] and the 1257 C.E. Samalas eruption[141].

Here I argue that the 1257 C.E. Samalas and the 1815 C.E. Tambora eruptions triggered rapid mutation of *Y. pestis,* and contributed to environmental conditions beneficial to its subsequent spread. This suggests a simple trigger for two of the most devastating pandemics of the Common Era, and potentially represents a new and previously overlooked consequence of explosive, halogen-rich volcanic eruptions.

4.2: Results

The results presented below represent three novel lines of enquiry: (1) Radiative reconstructions of previously identified key plague regions following the 2010 C.E. Merapi eruption and a discussion of scaling these results to represent the Samalas (1257 C.E.) and Tambora (1815 C.E.) eruptions, (2) Synthesis of previous historic research with the hypothesised event timeline presented in this thesis and, (3) Climatic (temperature and hydro-climatic) reconstructions of the key plague regions over the time period coincident with, a prolonged period of elevated GVF, the Samalas eruption and the suspected initiation of plague in Central Asia.

4.2.1: Volcanic ozone depletion and UV-B variation

4.2.1a: Historic precedent

High altitude areas receive elevated terrestrial doses of UV-B, and the Tibetan Plateau currently receives one of the highest doses globally[53] as illustrated by Beckman et al. (2014)[53] (**Figure 3b)**. Exceptionally high doses of UV-B would have irradiated the Tibetan Plateau during summer months following periods of ozone depletion, such as the years

after large volcanic eruptions. The Tambora and Samalas eruptions were exceptionally large, ejecting three to eight times (respectively) the sulphur dioxide as the Pinatubo eruption (**Table 2**), which had demonstrable effects on both atmospheric ozone and UV-B radiation rates. Both eruptions were high intensity Plinian (Tambora) or Ultraplinian (Samalas) events similar to the Pinatubo 1991 C.E. eruption. The Pinatubo eruptive column reached an altitude of greater than 40 km, whereas the Samalas eruptive column may have reached an altitude of 43 km and ejected a bulk deposit volume of 5.6-7.6 km^3 (minimum estimate)[142], compared to the 3.4-4.4 km^3 estimate for Pinatubo[143]. Sulphur dioxide injections into the stratosphere quickly forms the sulphuric acid (H_2SO_4) aerosol which contributes to increased scattering of incident radiation and a decrease in UV-B insolation. Sulphate aerosol surfaces provide sites for heterogeneous chemical reactions that activate halogen species and facilitate the destruction of ozone[134].

Eruption (Date C.E.)	**VEI**	**SO_2 (Tg)**	**Cl (Tg)**	**Estimated Ozone Depletion (%)**
Merapi (2010)	4	0.44[144]	-	Anomalous depletion at Mid – High Northern latitudes[145]
Pinatubo (1991)	6	20[130](18± 4-19± 4[146])	3[137]	2-7[130] (Tropics – Mid latitudes respectively)
Tambora (1815)	7	60[147] (73-91[141])	18-23[141]	Unknown
Samalas (1257)	7	158± 12[141]	227± 18[141]	20% (in areas of high aerosol concentration)[141]

Table 2. The SO_2, Cl and Volcanic Explosivity Index (VEI) of several key volcanic eruptions and estimates of associated ozone depletion from literature.

Samalas was the largest single sulphur injection event of the past seven thousand years[142] and Vidal et al. (2016)[141] suggest that it caused significant global ozone depletion. Both Samalas and Tambora are estimated to have had high halogen concentrations (**Table 2**), which would have significantly diminished stratospheric ozone concentrations. Several recent studies[128,139,148] suggest that the injection of hydrogen halides (e.g., HCl) could have delivered significant levels of halogens to stratospheric altitude which, combined with sulphate aerosols, could catalyse significant ozone depletion. Carn et al. (2016)[128,139] suggested a co-injection ratio of 0.014 for HCl:SO_2 which I calculate could potentially deliver 2.21Tg (Samalas) and 0.84Tg (Tambora) of HCl to stratospheric altitude assuming adequate HCl is available within the total Cl ejected, and trigger significantly larger ozone

depletion than the 1991 C.E. Pinatubo eruption[128]. Consequently, it is extremely likely that the years immediately following the Samalas and Tambora eruptions had the lowest atmospheric ozone concentrations and the highest terrestrial UV-B exposure of the last few thousand years.

4.2.1b: A case study: testing the effects of a moderate-sized modern eruption on UV-B radiation rates

The October-November 2010 Merapi eruption, which has a VEI of 4, sits within the operational window (2004 to Present) of NASA's Ozone Monitoring Instrument (Aura-OMI) which records erythemal daily dose (local noon) UV data globally representative of surface UV-B radiation. Merapi is located in Indonesia, approximately 675 km from Samalas and 840 km from the Tambora caldera (**Figure 3c**). The 2010 C.E. Merapi eruption was one of the largest within the Aura-OMI operational window and its location proximal to Samalas and Tambora makes it an ideal candidate to investigate how eruptions in this geographic area influence UV-B radiation rates over the Tibetan Plateau. The eruption was sub-Plinian and its eruptive column reached an altitude of 18.3 km[145,149], thereby reaching the stratosphere. Previous research identified mid-latitude ozone depletions and subsequent UV-B increases during the spring of 2011 C.E. over Tomsk (Russia) and Europe[150], and attributed these to aerosol input from the Merapi eruption[145], illustrating that even this moderately sized eruption did have consequences in terms of increased UV-B incidence rates.

Here I evaluate the UV-B shifts over the identified *Y. pestis* source region on the Tibetan Plateau (**Figure 4**) in response to the Merapi eruption. UV-B varies seasonally, with summer values significantly higher than winter values (**Figure 4a**)[53]. The maximum mean value (by month) across the source area was 10.015 KJm^{-2} in July 2011 (96.5°E, 30.5°N, **Supplementary Table 3**) with the highest values occurring early in July (4^{th}) (**Supplementary Figure 1**) .The South Western point within the source area (96.5°E, 30.5°N) is a small region of anomalously high UV-B, despite its moderate altitude in comparison to much of the Himalayas (3,499m). The only area of higher UV-B values within this region is the area of the Tibetan Plateau along the Nepal border encompassing Mount

Everest (**Supplementary Figure 2**). Much of the area of peak UV-B proximal to Mt. Everest is a potential natural foci of plague[151], with the himalayan marmot (*Marmota himalayana*) host populations observed close to this area[152]. However this region has never been discussed as a potential plague source and therefore warrants further investigation. July 2011 is the month of highest UV-B exposure across the entire observational window (**Figure 4b**). Additionally, UV-B spatial variation during this peak month (**Figure 4c**) shows strong association with *Y. pestis* host (himalayan marmot) and vector species[151] and georeferenced strain isolates[22] ; the majority of strains within the source area (including the 0.PE7 strain proximal to flea transmission acquisition) plot in a NE-SW trending central corridor bounded by the current monsoon limit and south eastern drop off in UV-B values.

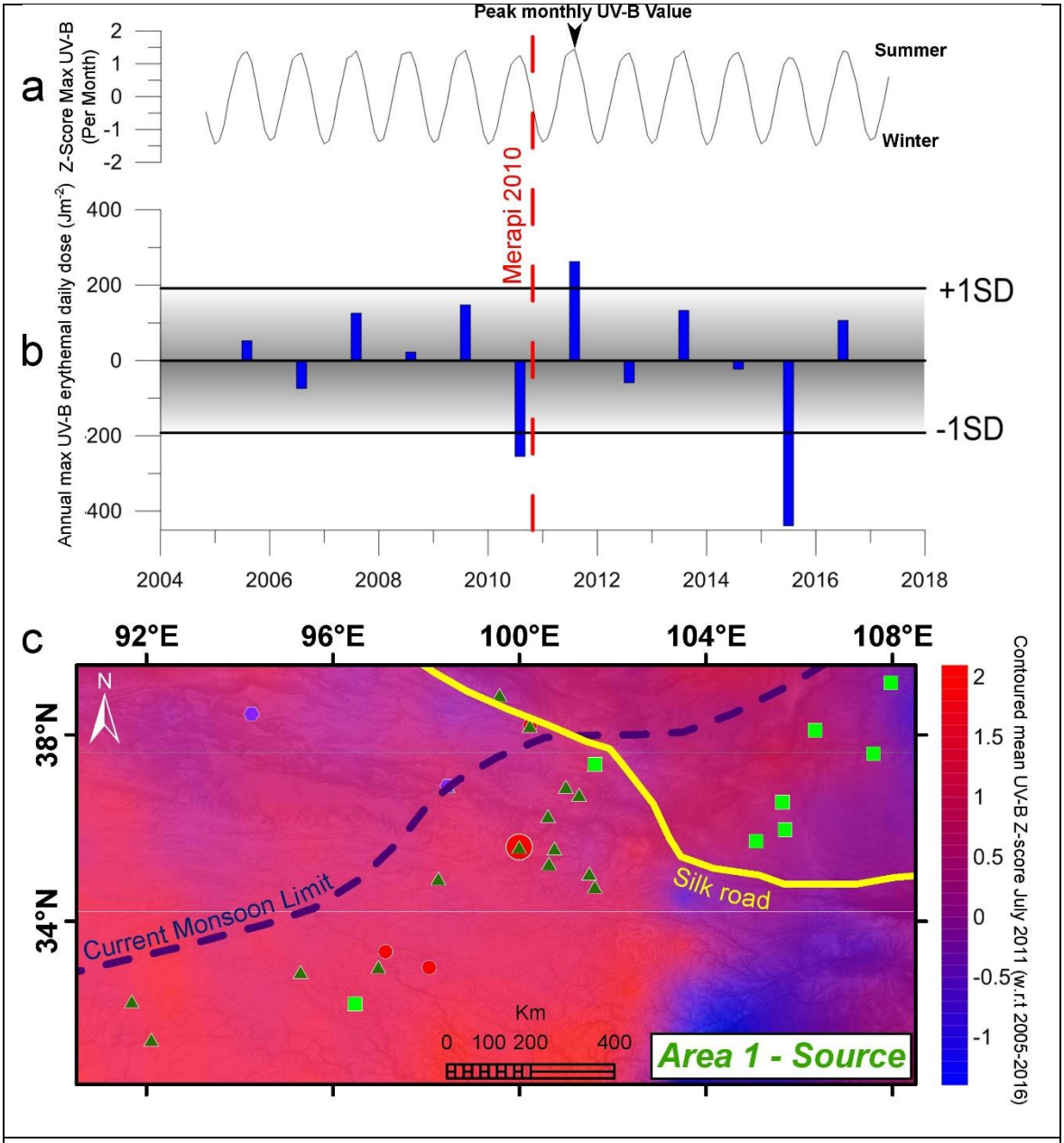

Figure 4. UV-B variation within the source area following Merapi (2010). (**a**) Seasonal variation in peak erythemal UV-B daily dose displayed as z-scores, with the summer following the Merapi 2010 C.E. eruption highlighted as highest value in the record. (**b**) Annual maximum UV-B erythemal daily dose values per month over twelve years highlighting the anomalously high UV-B doses during the summer immediately following the Merapi Eruption. (**c**) Contoured Z-score for the month of maximum UV-B exposure (July 2011) within the operational window of the Aura-OMI satellite for the source area. Highlights the trend in *Y. pestis* strain data to primarily plot between the furthest reach of the current monsoon limit and the area of rapid decrease in UV-B values to the South East.

The Tambora and Samalas eruptions dwarf the 2010 C.E. Merapi eruption in all respects. However, the Merapi eruption still caused appreciable ozone depletion[145,150] (Figure 4) and subsequent increases in UV-B across the Northern Hemisphere including the *Y. pestis* source area. Due to the geographic proximity of the Merapi eruption to the Samalas and Tambora eruption locations it is tempting to scale the stratospheric influences of Merapi described above to infer the potential influence of the VEI7 eruptions. The expected ozone depletion and subsequent increases in UV-B radiation following the

Samalas and Tambora eruptions should vastly surpass the effects following the Merapi eruption, especially in the source region. In other words, upscaling the effects of the VEI4 Merapi eruption to the VEI7 Tambora and Samalas eruptions would suggest substantial peaks in a known mutagenic element (UV-B) closely coinciding (within errors) with estimated polytomy dates (Samalas, 1257 C.E., N07 Polytomy, 1268 C.E.: Tambora, 1815 C.E., N14 Polytomy, 1808 C.E.)[22].

4.2.2: Historical Evidence

There is no mention of the Samalas eruption within Mongol records of the period. However English and Japanese records of the time suggest a period of famine following Samalas[38,39] and there is record of 'pestilence' in Syria[95], however no evidence suggesting influence of *Y. pestis*. The expansion of the Mongol empire began under Chinggis Khan (1206 C.E.) continuing until its eventual fragmentation into separate Khanates in 1294 C.E. following the death of Kublai Khan[79]. The majority of historical evidence suggests plague initiated in Central Asia in the mid 1330's[18,95]. This is followed by the first archaeological evidence of plague from Nestorian Christian grave sites proximal to Issyk-kul[17], after which plague is assumed to have spread west along the Silk Road until reaching the Genoese port city of Kaffa in 1346[3] and from there throughout Europe in the coming decade[91]. The Nestorian communities may have suffered significant hardships immediately preceding plague initiation, through raids from opposing Mongol Khanates[96], and continued religious oppression[79], placing them in a highly fragile state and more susceptible to infection through malnourishment[42]. This thesis argues that this period of societal trauma extending from around 1315[96] to late the 1330's[79] coincided with climatic conditions optimal for plague prevalence within this area.

The influence of the Mongol empire across Central Asia both preceding and coinciding with the period of the Black Death should not be understated, with an expansion in pan-Eurasian trade and an increased persecution of populations assumed pivotal to the initiation of plague both attributable to the Mongol empire. Mongol expansion and the increased use of far-reaching trade routes facilitated the transport of goods across Eurasia

and potentially the same networks enabled rapid dissemination of *Y. pestis*[79]. The early fourteenth century was a period of repeated and near constant warfare between opposing Mongol Khanates coincident with increased religious oppression of the Nestorian Christians until their eventual complete expulsion from Central Asia by the late 1360's C.E.[96]. Trade from Europe and the Middle East across Central Asia to China saw a boom in the 1320's C.E. and 1330's C.E. due to rapprochement between the Mongol Khanates[79]. This closely coincides with the Issyk-Kul grave sites (1338/9 C.E.)[17] and fragmentary evidence suggesting the incidence of plague within the Mongol empire at the start of the 1330's C.E.[18,95]. Following the initiation of the plague it is then plausible that Mongol military movement aided in transporting *Y. pestis* west eventually reaching the Black Sea port of Kaffa, the supposed passage of the plague into Europe[95]. The Mongol Empire may therefore have not only shaped the societal conditions which enabled *Y. pestis* to achieve zoonosis but also facilitated its transmission across Eurasia.

4.2.3: Thirteenth - fourteenth century volcanism and climate

The Asian summer (JJA) temperature reconstructions PAGES Asia 2K[61] and N-TREND (Eastern Eurasian Region)[63] were compared to verify the use of the higher spatial resolution (2°x2°) PAGES data set to reconstruct the source and zoonosis areas individually from 1200 to 1400 C.E. (**Figure 5**). At both annual and decadal (eleven year

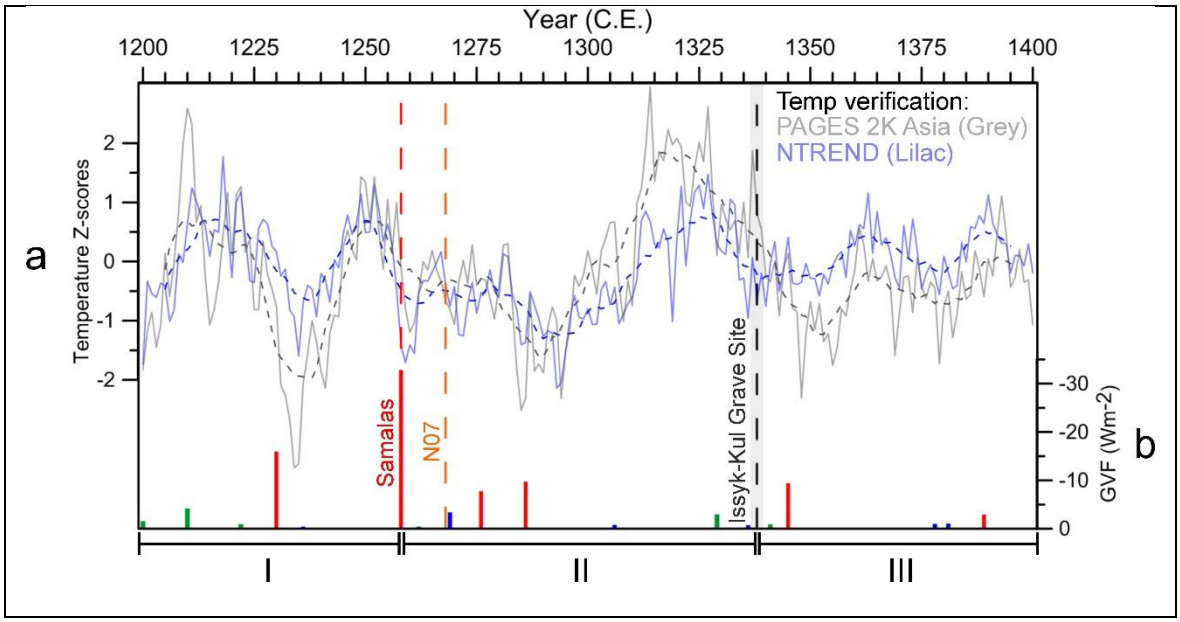

Figure 5. Comparison of Asian temperature reconstructions across the period of cooling following volcanic loading of the late thirteenth century. (**a**) Comparison of PAGES Asia 2K summer temperature reconstruction[61] with the N-TREND Northern Hemisphere summer temperature reconstruction for Eastern Eurasia[63] accompanied by eleven year running average values (dashed), separated into three periods of interest, I, II and III. Both reconstructions are presented as z-scores (w.r.t. 1750-1950 C.E.) (**b**) Global volcanic forcing estimates[44] separated by eruption latitude; Southern Hemisphere (blue), Northern Hemisphere (green) and tropical (red). The dates highlighted by dashed lines are; 1257 C.E. eruption (red), 1268 C.E. N07 polytomy[22] (Orange) and the 1338 C.E. date of the plague gravesites proximal to Issyk-Kul (Black).

running mean) timescales a good correlation exists between the two reconstructions, with PAGES consistently showing greater amplitude fluctuations. The 1200-1400 C.E. period is considered as three discrete sections for the purpose of this study (**Figure 5**).

I) 1200 – 1257 C.E.: This period shows consistent profiles in both records, with the highest temperatures occurring at around 1210 C.E., followed by an abrupt end to this period of warmth at 1228/29 C.E. This cooling may reflect a volcanic sulphate loading event identified at 1229 C.E. Based on ice core records, Gao et al. (2008)[153], Crowley and Unterman (2013)[154], and Sigl et al. (2015)[44] all identify this eruption (the latter study dates peak at 1229 C.E., former two dates peak at 1227 C.E.) however the eruption location is not currently known. The post 1229 C.E. cooling is the among the most substantial of the period considered in the PAGES data and is of a similar size to the post-Samalas cooling despite the fact that current GVF estimates associated with this eruption are less than half that of Samalas[44]. The N-TREND data suggest a smaller cooling trough, less than the cooling immediately following Samalas as would be expected. After the 1229 C.E. cooling event, both temperature reconstructions return to baseline values, before further cooling associated with the 1257 C.E. Samalas eruption.

II) 1257 – 1338 C.E.: The peak GVF associated with Samalas is dated to 1258 C.E. from ice core data[44], however the climate response to Samalas suggests an eruption in the summer of 1257 C.E.[47,141]. An eruption date of May – July 1257 C.E. is further supported by the reported arrival of a persistent dry fog over England in the late autumn of 1257 C.E.[37]. This may explain the apparent early cooling seen in both temperature reconstructions; cooling in the N-TREND data associated with the Samalas eruption is the largest and most rapid seen across this period of study. The PAGES data shows a cooling spike coincident with the 1258 C.E. date, however the magnitude of cooling is only moderate. PAGES

reaches a minimum at 1285 C.E. and N-TREND at 1293 C.E., representing the 11th and 13th coldest years of the respective records (PAGES Asia 2K 800 – 2009 C.E.; N-TREND 750 – 2011 C.E.). From this point both show a consistent rise in temperature with a slight perturbation to this increase at 1310 C.E. PAGES reaches a peak at ≈1315 C.E. with the N-TREND peak lagging about ten years and peaking at ≈1325 C.E. This peak in temperatures is a maximum in the PAGES annual reconstruction over the period of investigation (1200 - 1400 C.E.). The maximum in the N-TREND the peak equals previous maximum values for the period. Following peak values, each temperature reconstruction then shows a cooling trend before the Issyk-Kul grave site (1338 C.E.).

III) 1338-1400 C.E.: This final interval was characterised by the most stable temperatures in both datasets. The temperature reconstructions show general agreement over this period with a small discrepancy around the 1350's where PAGES shows a significant minimum, potentially associated with the 1344 C.E. sulphate spike, which is not visible in the N-TREND reconstruction.

The temperature fluctuations in Interval II are most relevant to the Black Death pandemic. Both temperature reconstructions were well-correlated over this interval, supporting the application of the PAGES Asia 2K reconstruction at a higher spatial resolution. The PAGES reconstruction was therefore used to identify temporal and spatial variability in temperature across the source and zoonosis areas (**Figure 3a**) in the period of most interest, 1250-1350 C.E. (**Figure 6**).

Both records suggest considerable and immediate cooling post-Samalas lasting 3-4 years followed by an initial partial recovery. Following Samalas three further moderate (3-10 Wm^{-2} GVF) eruptions are identified in bipolar ice core records in quick succession. Both areas show maximum cooling within this period (1250-1350 C.E.) at 1285 C.E which I estimate represents a summer mean temperature of 12.2°C in the source area and 19.0°C in the zoonosis area. The individual cooling contribution of each eruption is difficult to determine. Recent analysis suggests that post volcanic cooling for an eruption on the scale of Samalas could supress global temperatures for greater than ten years[44], separate eruptions within

this period may further suppress temperature or alternatively elongate cooling. The thirteenth century represents a prolonged period of sustained volcanic forcing therefore the regular replenishment of volcanic aerosols may prolong the cooling. Alternatively this may represent local temperature responses to the influence of ocean atmosphere feedbacks suggested to have contributed to long term cooling and the initiation of the LIA following late thirteenth century volcanic loading[45]. Temperature trends for the areas diverge following the temperature minimum in 1285 C.E with the zoonosis area initiating a period of intense warming while temperatures continued to decrease in the source area. A forty-year period of sustained anomalous warmth (**Period X - Figure 6**) within the zoonosis area peaks in 1318 C.E. and 1319 C.E. with a temperature high of 23.1^{o}C, the warmest values from this area across the entire 1,200 year record. The temperature optimum for the oriental rat flea (*Xenopsylla cheopis*), a primary vector for bubonic plague is 20-30°C[24]. The temperature within the zoonosis area changes from 19°C at the post-volcanism temperature minimum, outside of the functional range of *Xenopsylla cheopis*, to 23°C during the peak warming in period X, which is within the functionally optimal range. This may have influenced the timing of the zoonosis event. The end of period X coincides with the first archaeological evidence of human plague victims (1338 C.E. in Issyk-Kul).

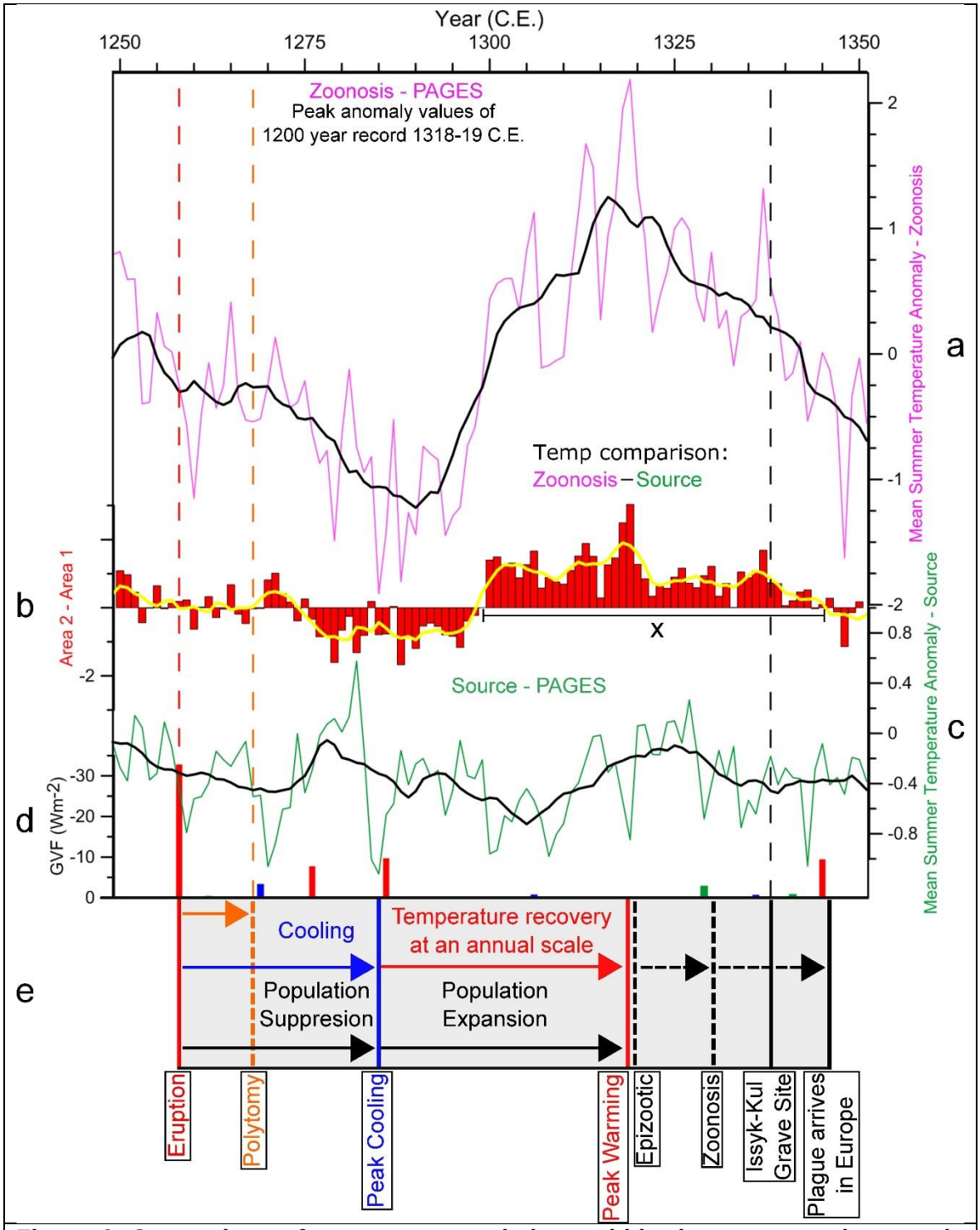

Figure 6. Comparison of temperature variations within the source and zoonosis areas across the period of the Black Death pandemic. (**a**) Mean summer temperature anomaly across the zoonosis area (PAGES Asia 2K) with 0 equivalent to 20.9°C. (**b**) Comparison of mean summer temperature anomalies of the source and zoonosis area, (**X**) Roughly 40 year period of intense and persistent warming within the zoonosis area, encompassing the two warmest years in the zoonosis area over the complete record (1318-19 C.E.). (**c**) Mean summer temperature anomaly across the source area (PAGES Asia 2K) with 0 equivalent to 13.3°C. (**d**) Global volcanic forcing estimates[44] separated by eruption latitude; Southern Hemisphere (blue), Northern Hemisphere (green) and tropical (red). (**e**) Schematic representation of the presented hypothesis with dates of the Samalas eruption[142], peak predicted cooling, peak recovery warming temperature, Issyk-kul grave site and *Y. pestis* arrival in Europe illustrated with solid lines. Estimates of the 'Big Bang'[22], *Y. pestis* epizootic within rodent populations, zoonosis and pandemic spread are illustrated with dashed lines. Internal labelling of arrows represent temperature variations and expected host and vector population responses with respect to trophic cascade[32].

Warm and wet periods correlate with increased plague prevalence through their influence on *Y. pestis* host populations over long timescales[5,30,33]. Hydroclimate reconstructions are therefore necessary when attempting to estimate ideal conditions for epizootic periods within host populations. The intense and geographically isolated warming within the zoonosis area in the years 1318-1319 C.E. coincides with variable but generally wet years determined through PDSI values[62], within the zoonosis area coinciding with, and immediately following peak temperatures (**Figure 7**). A smaller annual peak in temperature coincided with the Issyk-kul grave site date of 1338 C.E. This latter temperature peak is also associated with a substantially wet period within the zoonosis area. This suggests that climatic conditions were optimal for plague during the peak warming years of 1318/19 C.E. as well as the grave site date of 1338 C.E. within the zoonosis area. Plague may have achieved zoonosis proximal to Issyk-Kul in 1318/19 C.E. but is only identifiable in 1338 C.E. several years later due to the temporal resolution of archaeological evidence in the area.

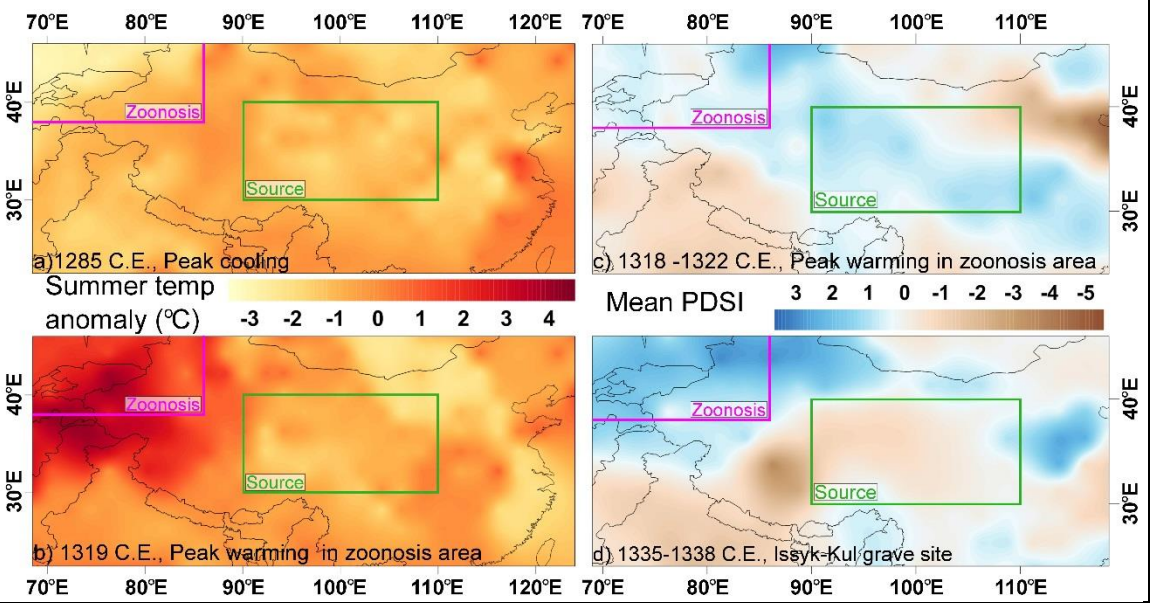

Figure 7. Contoured summer temperature anomaly and PDSI maps across short term periods of interest for *Y. pestis* host and vector populations. The left hand panels represent contoured temperature reconstructions[61] for the date of peak cooling following the volcanic forcing period in the source and zoonosis area (**a**) 1285 C.E. and the peak warming of the recovery period within the zoonosis area (**b**) 1319 C.E. The right hand panels represent contoured PDSI reconstructions[62] from the period of peak warming within the zoonosis area (**c**) 1318-1322 C.E. and the period of the Issyk-kul grave site as well as a significant later warming peak (**d**) 1335-1338 C.E.

4.2.4: Synthesis

The 1257 C.E. Samalas eruption may have catalysed a key mutation of the *Y. pestis* bacteria through the process of halogen aerosols negatively influencing atmospheric ozone,

thereby increasing UV-B incidence rates and mutagenesis. Climate change caused by repeated reinjection of volcanic aerosols from Samalas and several smaller temporally proximal eruptions initially suppressed (through cooling) and then promoted (through warming recovery) the spread of *Y. pestis* bacteria contributing to the zoonosis event, and eventually leading to the Black Death pandemic (**Table 3, Figures 4-7**). Previous work suggested that prolonged elevated GVF contributed to global climatic cooling such as the LALIA[43] and the LIA[45] through sea-ice/ocean feedback mechanisms. This cooling caused societal upheaval likely to have had a positive impact on the prevalence of disease, we therefore suggest that volcanism further contributed to the longevity of plague pandemics and that isolated large eruptions may not have an impact of comparable scale. This study presents a possible chain of events from the Samalas eruption through the period of intense GVF to the initiation of the plague pandemic and the ensuing progress to medieval European populations (**Figure 6e**). The hypothesis suggested consists of a four key processes:

1) **Volcanic halogen aerosol-induced ozone degradation:** An extremely large explosive volcanic eruption contributes to ozone depletion and subsequent UV-B radiation increases. These increases are particularly severe over areas of high altitude, greatly promoting mutagenesis in an environment that harbours *Y. pestis* host populations. The N07 polytomy is predicted to have arisen immediately following the Samalas eruption.
2) **Post-volcanic cooling:** The 1257 C.E. eruption of Samalas combined with several other large eruptions contributed to a sustained period of elevated Global Volcanic Forcing (**Figure 8**) and associated cooling. Temperature strongly influences *Y. pestis* host and vector populations on the Tibetan Plateau (predominantly Himalayan marmots) and consequently regional plague prevalence[151]. This sustained cool period may therefore suppress populations and limit the expansion of the newly diverged *Y. pestis* strains later responsible for the Black Death pandemic episode.

3) **Host population expansion:** Temperature recovery following volcanic perturbation will benefit host populations and aid in the spread of *Y. pestis* bacterium. Human populations further promote dissemination through trade routes (Silk Road) proximal to *Y. pestis* source regions[22] and Mongol military movements. Warming within the zoonosis area moves temperatures into optimum functional range for the common plague vector *Xenopsylla cheopis* between 20-30°C. This is concurrent with times of significant hardship for human populations local to Issyk-Kul through damage to agricultural land[96] and religious suppression[79]. Preferential conditions for plague and transport via the Silk Road may have allowed Y. pestis to reach the identified zoonosis area, in which climate and societal unrest may have facilitated a rapid epidemic episode, which subsequently developed into the Black Death pandemic.

4) **Societal impact of prolonged cooling period:** Population health impacts disease prevalence with undernutrition a leading risk factor[155]. Periods of prolonged elevated GVF may contribute to global cooling[43,45], which in turn will have impacted crop growth and may have contributed to further societal unrest enabling *Y. pestis* to have had such a significant and prolonged impact[3] through each pandemic episode.

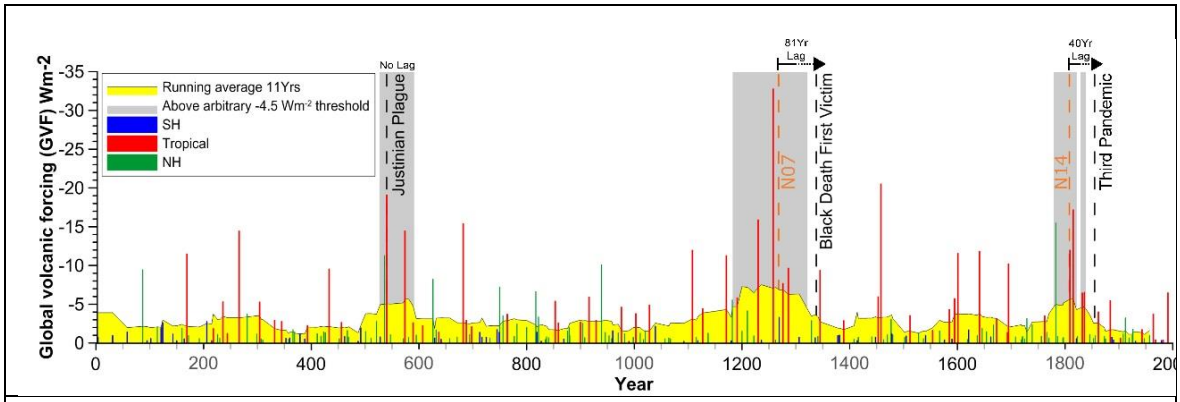

Figure 8. Volcanic forcing correlated with major plague pandemics. Global volcanic forcing estimates[44] separated by eruption latitude are shown; Southern Hemisphere (blue), Northern Hemisphere (green) and tropical (red) with an eleven year running average of all eruptions (yellow). Earliest evidence of fatalities during pandemic episodes illustrated (black dashed), respectively; Justinian Plague in 540 C.E.[1], Black Death in 1338 C.E.[17,79] and the Third Pandemic in 1855 C.E.[156]. Peaks in the running average correlate with each pandemic episode, this is highlighted by grey boxes which illustrate when the running average surpasses a -4.5 Wm^{-2} global volcanic forcing value. The lag between the estimates of polytomy date and pandemic initiation are represented by black arrows.

4.3: Discussion

4.3.1: Volcanism induced mutagenesis

In this chapter I discuss the potential for thirteenth century volcanism, specifically the 1257 C.E. Samalas eruption, to: I) reduce stratospheric ozone triggering mutation of the *Y. pestis* bacteria, II) cool climate resulting in isolation and suppression of the host population, and III) the return to warmth promotes expansion of the host population, zoonosis, and exposure to humans along the Silk Road. However, the process described here triggered by the Samalas eruption was not an isolated event, and any large, halogen-rich eruption could have similar repercussions. For example, the 1815 C.E. Tambora eruption should also have triggered a similar mechanism, and in fact Tambora shows close association with: i) the N14 polytomy (1808 C.E, 95% CI 1142-1338 C.E.[22]), ii) a prolonged period of global cooling[44], and iii) subsequent recovery warming, **(Supplementary Figure 3**) culminating in the initiation of the Third Pandemic of *Y. pestis* in the 1850s within the recently beleaguered populations of Yunnan province[15,103].

Other examples of volcanogenic ozone depletion causing periods of increased mutagenesis by increasing UV-B flux exist in the literature[54,55]. For example, halogens released during the eruption of the Late Permian Siberian Traps may have led to ozone depletion, an increase in UV-B radiation, and consequently the development of mutated palynomorphs[54]. This provides an example of ozone depletion contributing to mutation, however over a much longer time interval (100-600 thousand years) and influencing a much broader range of organisms. A similar example of volcanically induced ozone depletion contributing to increased mutagenesis may have occurred in tropical forests of the Eocene. Eocene palynomorphs show a rapid increase in diversity which may have been caused by a combination of Milankovitch cycles contributing to regular warming phases driving Eocene megathermal forest taxa to higher altitudes and extensive volcanic eruptions in Greenland. This combination of high altitude and volcanically driven ozone depletion inducing increased UV-B radiation may have caused the increase in diversity observed[57]. Further studies discuss uplift as a potential control on UV-B radiation and provide further evidence of this mechanism causing speciation[55]. These studies illustrate a common relationship between increased UV-B and mutagenesis, specifically polytomies. For example, polytomies

associated with the uplift of the Tibetan Plateau[157] illustrate the mutagenic influence of UV-B, because no additional niche environments were created, but instead the whole region was lifted to a higher altitude. Sympatric speciation following such an event[157] is therefore definitively linked to increased UV-B flux rather than the exploitation of new ecosystems[55].

4.3.2: Differing circumstances of the Justinian Plague

The Black Death and the Third Pandemic represent two of the three known plague pandemics; the Justinian Plague of 540 C.E. is the third. The Justinian plague had an estimated death toll of at least 25 million[1], redressed economic power across Europe and coincided with the rise and fall of several Eurasian Empires[43]. Like the Black Death and the Third Pandemic, the Justinian Plague also occurs during a period of elevated GVF (**Figure 8**), however no lag exists between the largest forcing event and the pandemic initiation. The Justinian Plague is not associated with a polytomy or alteration in fixation rate immediately preceding the pandemic, and therefore is not directly applicable to the hypothesis suggested in this study. The first recorded deaths of the Justinian Plague are from the North African port city of Pelusium, after which *Y. pestis* spread to the trading hub of Alexandria before further spreading widely across the Mediterranean. The combination of an unconfirmed African source region and the influence of volcanic cooling may have facilitated the initiation of this pandemic episode. Cooling following the mid sixth century sulphate spikes may have sufficiently lowered temperatures across East Africa to allow transmission of *Y. pestis* from the potential source region in the kingdom of Aksum (Ethiopia).The volcanic cooling may have allowed infected hosts and vectors to survive the northwards journey from East Africa to Pelusium; the temperatures experienced in transit would usually be beyond the tolerable range of vectors during post-harvest transport (33-40˚C). *Y. pestis* may have spread from the possible East African source area to Pelusium where the Justinian Plague began[1,24]. However, recent genetic studies suggest Central Asia as the source region for the Justinian strain at the beginning of the Common Era (4 C.E., HPD interval 400 B.C.E. – 315 C.E.)[23]. Therefore, an African origin for the Justinian Plague would require prior transport of the strain from Central Asia to sub-Saharan Africa. Ancient Chinese-African trade routes are not known, with the oldest documented routes only active

since the ninth century[158]; evidence for earlier trade routes would therefore provide support for East African plague genesis.

4.3.3: Human influence on pandemic initiation

Evidence exists that conflict and subsequent ill health following the Mohammedan Rebellion of 1855 C.E. in Yunnan province may also have helped initiate the Third Pandemic [15,26], similar to the conditions suffered by the Nestorian Christian populations proximal to Issyk-kul prior to the Black Death through the progressive Islamization of the Western and Central Khanates[79]. Both the Black Death and the Third Pandemic show the first recorded victims in close association with areas of the conflict, which introduces a human factor that is difficult to quantify. In the case of the Black Death the Mongols not only contributed to conflict in key areas but also facilitated the potential transport of *Y. pestis* from these regions through a combination of increased Eurasian commerce and military movement. This final step in the initiation of plague pandemics illustrates the complexity of such events. Bos et al. (2011)[19] suggest that plague pandemics are caused by a constellation of factors including: genetics of host populations, vector dynamics, social conditions and influence of concurrent diseases, with several other studies showing the influence of climate on the host regions[29,30,33,151,159,160]. This study suggests the addition of global volcanic forcing and its influence upon UV-B levels and climate as well as social factors influencing proximal human populations as further influential factors.

4.3.4: Exploring the Null hypothesis

This thesis has predominantly accepted the assumption that the polytomies prior to the second and third pandemics are associated in some way with pandemic outbreaks, however the alternative must also be explored for several reasons. Firstly there is no consensus that the 'Big Bang' influenced the virulence of *Y. pestis*, so the potential epidemiological impact of plague is not known to be different immediately before or after the event. Zimbler et al. (2015)[12] tentatively suggest that a genetic adaptation which enhanced the invasive capacity of *Y. pestis* during bubonic plague may have influenced the 'Big Bang'. This suggests the following chain of events: a genetic change occurred, leading to an epidemic within host populations, which can be assumed to also be climatically

modulated[60], which is not incongruous with the volcanically modulated hypothesis suggested here.

A further issue with the polytomy is the very broad confidence level in the molecular clock estimations, with Cui et al. (2013)[58] stating a 197 year range within the 95% confidence level. Rasmussen et al. (2015)[21] does not suggest a polytomy but instead several rapid divergence events with a huge overlap in 95% highest posterior density interval, with the emergence of branches 1-4 (Figure 2) (synonymous with the 'Big Bang') covering a collective period of 355 years (901 C.E. – 1256 C.E.). This highlights the huge potential error and variance in molecular clock calculations. Wagner et al. (2014)[23] further questions the validity of molecular clock date estimates for the *Y. pestis* genome, as the highly variable fixation rate observed within *Y. pestis* may lead to erroneous estimates. The final flaw is that the Justinian Plague does not appear to be associated with a similar polytomy or a huge increase in fixation rate setting it apart from the later pandemics.

If genetic data is disregarded this thesis must instead ask if volcanism had significant further influence upon pandemic episodes to warrant inclusion in historic plague models. The climatic reconstructions of the source and zoonosis areas in this study suggest that, immediately prior to the Black Death, climatic conditions became favourable to plague prevalence through increased temperature and precipitation. The dramatic warming within the zoonosis area before the Black Death, when viewed in combination with Kausrud et al.'s. (2010)[5] warning of increased plague risk in this area under future warming conditions suggests the regional climatic conditions were pivotal to pandemic initiation. This thesis suggests that these conditions were heavily influenced by volcanism. The cooling culminating in 1285 C.E. was arguably modulated by the prolonged period of volcanic forcing with subsequent warming potentially representing a brief recovery period (Figure 6) prior to the prolonged cooling of the LIA, also potentially driven by volcanism[45]. If volcanism is assumed to have modulated these climatic conditions then its impact on the plague is easily reconciled, having contributed to conditions which increased plague prevalence in its central Asian source region and then influenced changing societal conditions through the

LIA. The Justinian plague similarly coincides with volcanically mediated prolonged climate change (LALIA)[43] which may have influenced the Justinian plague across its several century span at least within Western Eurasian populations.

Periods of elevated volcanism have repeatedly coincided with plague pandemic episodes. These periods of volcanism will have had significant climatic impact and subsequently influenced ecological and societal change (Figure 9). The eruptive periods preceding each pandemic largely agree with the presented hypothesis. The mid-late thirteenth century eruptions (including Samalas) likely contributed to ozone depletion through stratospheric sulphate and halogen injection (**1**)**,** contributed to cooling and recovery warming in an area pivotal to plague ecology (**2**), and may have influenced long term climatic change contributing to the initiation of the Little Ice Age[45] (**3**). The combination of the 1809 and Tambora eruption will have produced similar stratospheric injections (**1**), followed a similar cooling and recovery pattern (**2**) and contributed to significant societal upheaval in Yunnan province (pivotal to third pandemic) and a prolonged period of cooling due to positive feedback mechanisms is plausible[43,45](**3?**). The eruptive period coincident with the Justinian plague may have contributed to prolonged climatic and societal change[43] (**3**), further investigation is required to ascertain whether the other factors (**1, 2**) are satisfied. The 1452/53 Kuwae (Vanuatu) eruption may have caused substantial stratospheric injection leading to ozone depletion[161] however the temporal isolation of the eruption may

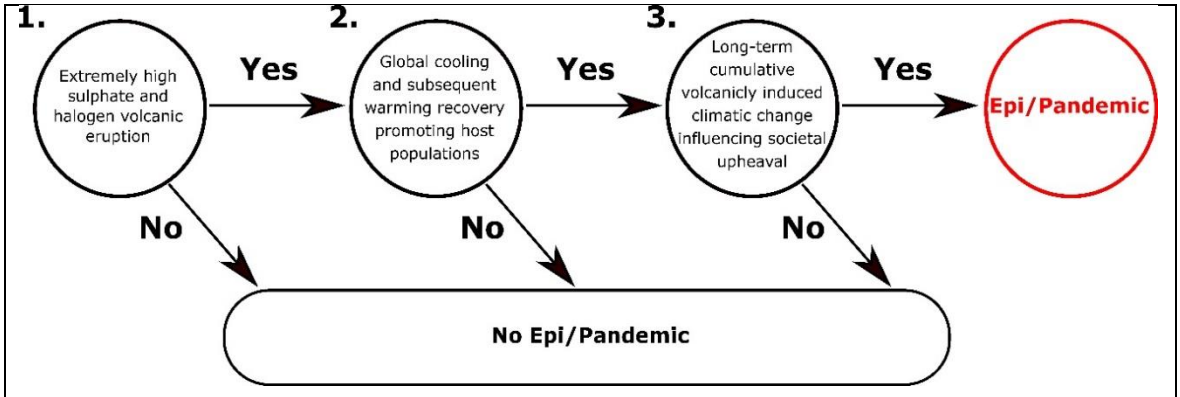

Figure 9 | Schematic flow diagram of the presented hypothesis linking a single large high sulphur and halogen eruption, within a sustained period of volcanism to the initiation of Plague Epi/Pandemics.

explain the lack of apparent association with a plague epi/pandemic. Even when excluding the potential influence of radiative changes on bacterial evolution, volcanism appears to have contributed to each pandemic episode and therefore warrants further discussion in palaeoecological, epidemiological and historic research of past plague pandemics.

4.4: Conclusion

Stothers[37,38] suggests a link between the significant volcanic eruptions identified through sulphate loading in ice cores and pestilence, and in some cases 'Plague' of the last two millennia. The unidentified 536 C.E. eruption closely coincides with the initiation of the Justinian Plague, which is now genetically confirmed as *Y. pestis*[23]. The Stothers' 'unidentified 1258 C.E. eruption' (the 1257 C.E. Samalas eruption[142]) was linked to epidemics across Syria, Southern Turkey and Iraq (tentatively suggested to be plague) as well as pestilence across Europe causing "chilliness and listlessness that could last several months". This study works to revise the links suggested by Stothers and provide a mechanistic pathway linking significant explosive volcanic eruptions to initiation of genetically confirmed *Y. pestis* plague pandemics. The mechanism suggested here is well supported by previous studies, but would benefit from further research across a broad range of disciplines.

The polytomy estimates provided by Cui et al. (2013)[22] were constructed using the molecular clock method, which relies upon data acquisition across a varied timescale to calibrate points of divergence. Rasmussen et al. (2015)[21] completed a similar analysis producing a date estimate for the strain responsible for the Black Death of 901 – 1343 C.E (95% HPD) which is broader than the range suggested by Cui et al. (2013)[22] yet includes further calibration points from archaeological genetic data. Contrary to this, further genetic calibration points from plague burial sites – ideally temporally proximal to the divergence of relevant strains – should aid in providing better estimates as well as improvements in molecular clock methodology.

Current uncertainty regarding co-injection of hydrogen halides to stratospheric altitude should diminish through increased in-situ eruption sampling achievable through aircraft mounted monitoring systems, which suggested little evidence of HCl scavenging

following the Hekla eruption of 2000 C.E[162]. This should further aid model systems in predicting ozone depletion following eruptions outside of the influence of the industrial era[128].

Ultraviolet radiation, primarily UV-B can induce mutagenesis within bacterial communities through DNA damage which triggers genetic SOS repair systems[163]. This is regularly studied within *E. coli* which is a gram negative bacteria similar to *Y. pestis* and conjugative genetic transfer occurs between the two species in the flea mid-gut environment; *Y. pestis* may therefore exhibit a similar mutagenic response to UV-B exposure. High altitude bacterial communities regularly exhibit UV-B resistance which contributes to improved survival rate following UV-B exposure. Increased mutagenesis rates are also observed but not consistently throughout all bacteria[164]. Further experimentation upon a range of strains of *Y. pestis*, individually as well as in association with vectors, would therefore be hugely beneficial to this study.

Warm and wet conditions and their contributory effects on local vegetation are associated with increased plague prevalence particularly in association with the Black Death and the Third Pandemic[5,30,33]. This is easily reconciled with the 'trophic cascade' hypothesis over varying geographical and temporal scales but requires further rigorous testing under field conditions[165]. Annual scale variation and seasonality are however harder to integrate when looking at historical outbreaks. Evidence across Central Asia, predominantly from the area to the South of Lake Balkhash, suggests plague hosts and vectors reach dangerous threshold levels in response to spring warming and increased summer precipitation[30], therefore further inclusion of seasonal climatic conditions will improve accuracy of future reconstructions.

The complex progression of *Y. pestis* through a variety of hosts and vectors provides further uncertainty. A wealth of studies investigating the influence of climate upon plague prevalence focus on the great gerbil (*Rhombomys opimus*) and its associated vector populations within the Balkhash area of Kazakhstan. These studies provide detailed models of climatic influence upon the spread of plague[5,30] which show the expected peaks during

reconstructions of the historic pandemics. However the geographic range of these studies needs to be further assessed and investigation of alternate host species across a range of localities[166,167] would provide transferable evidence for other populations. The 'trophic cascade' hypothesis is conversely widely applicable but provides only a broad estimate of the response of *Y. pestis* associated host populations. Improvements could be made through ecological modelling of several key species of both hosts and vectors to ascertain the exact response to varying climatic and radiative conditions across a range of environments.

All three major plague pandemics of the Common Era occurred within times of significant and prolonged global volcanic forcing (**Figure 7**). Two of the pandemic episodes coincide with polytomy events within a few decades of the largest individual volcanic sulphate injections recorded. Previous studies have suggested links between climatic perturbations leading to warm and wet conditions and the initiation of pandemic episodes. This study illustrates that these suggested ideal conditions occurred in areas associated with initial plague pandemics preceding the available archaeological and documentary evidence (**Figures 1, 5-7)**. Additionally, a mechanistic pathway is suggested linking sulphur and halogen rich volcanic eruptions to genetic divergence events essential to the two most recent plague pandemics. Historic re-analysis has further shown dramatic similarities between the demographics of human populations associated with initial infection of *Y. pestis*, which warrants further investigation.

The hypothesis presented here not only suggests a mechanism for the initiation of past plague pandemics, but also highlights further risks of explosive halogen rich eruptions. Volcanic induced ozone depletion contributing to mutagenesis is not a new hypothesis[54,55,57], however it is seldom applied in a modern or historical context. In an era where antibiotic resistance is becoming more common[168], and epidemics of vector borne diseases such as Zika and Ebola are regular occurrences, knowledge of previous pandemic episodes may prove pivotal in mitigating future risk. Volcanic eruptions and subsequent climatic responses have regularly influenced human civilisations on varying time-scales[34,35,45]. The potential link between volcanism and the evolution of harmful bacterial

strains warrants further investigation, particularly in the current period of anthropogenically suppressed ozone concentrations[51]. The effects of a large, halogen rich eruption superimposed onto modern baseline (anthropogenically-modified) atmospheric halogen concentrations is unknown, but is worthy of considerable future investigation.

Chapter 5: Overall Conclusion

This thesis presents evidence supporting a mechanistic pathway linking periods of prolonged high global volcanic forcing, encompassing at least one sulphur and halogen rich explosive Indonesian eruption with major historical plague pandemics. The 1257 C.E. Samalas and 1815 C.E. and 1809 C.E. Tambora and unknown (respectively) eruptions may have depleted global ozone leading to increased fluxes of a known mutagenic element, UV-B. This effect is particularly prevalent at high altitude areas such as the Qinghai-Tibetan Plateau. This is the likely source region of *Y. pestis* and an area associated with a rapid genetic diversification event estimated to have occurred within just over a decade of the Samalas eruption. A similar period of rapid diversification may have occurred in close association with the 1815 C.E. Tambora eruption (and the 1809 unknown tropical eruption) contributing to the initiation of the Third Pandemic. These volcanic eruptions occurred in close association with several other eruptions causing prolonged periods of cooling and subsequent 'recovery' warming. This may have initially suppressed host populations before allowing expansion during a phase of temperature recovery through 'trophic cascade'. Following Samalas, this thesis illustrated such a climatic response, with the area of first archaeological evidence of plague within a human population (Issyk-kul) achieving peak warming and ample precipitation twenty years prior to the 1338 C.E. grave site. This strongly suggests that plague had the potential to achieve zoonosis two decades prior to the first archaeological evidence, which is highly plausible due to the limited availability of archaeological data. The human influence upon the zoonosis event is not fully resolved, with historical evidence suggesting that the first human victims of the Black Death and Third Pandemic were both from oppressed communities. These communities were likely poorly nourished and therefore sensitive to infections due to inhibited immunities. This factor warrants consideration especially when reassessing plague risk in the future with water and food shortages expected to increase. The Black Death and the Justinian plague both coincide with periods of global climatic change and subsequent regional societal upheavals (Little Ice Age and Late Antique Little Ice Age respectively) linked to prolonged periods of elevated global volcanic forcing. This highlights the potential impact of extended periods of

volcanism upon plague systems and thus society not just through the impact of individual large eruptions as previously discussed.

The Justinian Plague is not immediately preceded by a rapid diversification event, with the extinct strain responsible hypothesised to have diverged around the turn of the millennia (~500 years earlier). It is therefore not compatible with the mechanism proposed for the later pandemics. However, the timing of this early pandemic is coincident with a period of elevated volcanic forcing which previous studies have suggested may have enabled the transmission of *Y. pestis* from an already extent reservoir in East Africa. Much further work is required to confirm an East African source region and determine the potential influence volcanic cooling may have had upon subsequent *Y. pestis* transmission routes.

This thesis suggests that volcanic eruptions may have played a pivotal role in historic plague pandemics through aerosol emissions influencing UV-B radiation values and climate across regions pivotal to *Y. pestis*. The proposed mechanism linking large scale volcanism to UV-B radiation and therefore diversification may have influenced evolutionary progression of certain plant species through geological time. This thesis suggests that the same mechanism may have the potential to influence bacterial communities over much shorter timescales. This may have played a significant role in bacterial evolution over not only geological timescales but also on timescales affecting human development through the potential influence upon disease as demonstrated here.

Appendices

Supplementary Table 1. Fatalities from the western world during the 3rd pandemic[14]

Region	Total Fatalities
Central and South America	30,000
Europe	7,000
USA	500

All data from Echenberg (2002)[14]

Supplementary Table 2. Standard Error of mean temperature values across the total PAGES Asia 2K area, the source and zoonosis area.

Dataset and area	Standard Error in mean temp		
	Full length reconstruction	1200 C.E. – 1400 C.E.	1250 C.E. – 1350 C.E.
PAGES Asia 2K	0.007	0.02	0.03
PAGES Asia 2K: Zoonosis	0.02	0.06	0.08
PAGES Asia 2K: Source	0.01	0.03	0.03

Supplementary Script 1. Erythemal daily dose UV source area data extraction (example from June 2016)

```
library(ncdf4)                    # Opening needed package
setwd("H:/GEOL/Plague/Data/UV-B/Gionvanni plots/mydir")        #Collecting Data
ncname <-
"Merapi/2016/g4.timeAvgMap.OMUVBd_003_ErythemalDailyDose.20160601-
20160630.90E_30N_110E_40N"              #Set name of the NetCDF file, which in this
case is the data for June 2016
ncfname <- paste(ncname,".nc", sep="")
ncin <- nc_open(ncfname)
print(ncin)                    # Open and print the NetCDF file, showing variables,
dimensions and global attributes
lon <- ncvar_get(ncin,"lon")
nlon <- dim(lon)
head(lon)
lat <- ncvar_get(ncin,"lat",verbose=F)
nlat <- dim(lat)
head(lat)                      # Read latitude and longitude listing the first 6 values
print(c(nlon,nlat))            # Print the number of longitude and latitude values within
the file
title <- ncatt_get(ncin,0,"title")
institution <- ncatt_get(ncin,0,"institution")
datasource <- ncatt_get(ncin,0,"source")
references <- ncatt_get(ncin,0,"references")
history <- ncatt_get(ncin,0,"history")
Conventions <- ncatt_get(ncin,0,"Conventions")          # Get the attributes from file
attributes(ncin$var)$names                  # State the names of available
attributes
ncvar_get(ncin,"OMUVBd_003_ErythemalDailyDose")
x <- ncvar_get(ncin,"OMUVBd_003_ErythemalDailyDose")      # Prints all
Erythermal Daily Dose data within the file matrix
t(x)
max(x)                         # Print max value from Erythermal Daily Dose data

mean(x)                        # Print mean value from Erythermal Daily Dose data
median(x)                      # Print median value from Erythermal Daily Dose data
```

Supplementary Script 2. Temperature calibration extraction script written in bash (Unix shell)

```
#!/bin/bash
#
# Script: "extract_temp_data.sh"
#
# Purpose: to extract data at specific times/places from climate data file
#
# E GREGORY 18/07/2017 for H FELL

#
#-------------------------------------------------------------------------------
# FILE INFORMATION

# file format: ascii file called "cru_ts_3_10.1901.2009.tmp.dat"
# file format: 360 lines of data for every month, starting from Jan 1901, to Dec 2009.
# file format: 720 columns in each line, as for every month, there is a data point per grid cell for a 720x360 size grid.
# file format: not-a-number datapoints are indicated by -999

lpy=4320                # lines per year
lpm=360                         # lines per month
year0=1901              # first year in dataset

scalar=0.1              # scalar to apply to data in file (data is x 10 real temp value)

#
#-------------------------------------------------------------------------------
# CHOOSE TIMES TO EXTRACT DATA

echo -e "\n******** FILTERING BY TIME ********\n"

# years: 1951 - 1989
yearmin=1951
yearmax=1989

# months: June, July & August
monthmin=6
monthmax=8

#Creating loop to extract from for chosen years and months

year=$yearmin

datafile=year"$yearmin"-"$yearmax"_month$monthmin-$monthmax.dat

rm $datafile

while [[ $year -le $yearmax ]]
do

yearstart=`echo "$lpy $year0 $year" | awk '{print ($1*($3-$2))+1}'`

monthminstart=`echo "$yearstart $monthmin $lpm" | awk '{print $1+(($2-1)*$3)}'`

monthmaxend=`echo "$yearstart $monthmax $lpm" | awk '{print ($1+(($2)*$3))-1}'`
```

```
echo "*** YEAR = $year *** Line numbers: yearstart=$yearstart
monthminstart=$monthminstart monthmaxend=$monthmaxend"

# Extract data

awk -v LINEMIN=$monthminstart -v LINEMAX=$monthmaxend '{if (NR>=LINEMIN &&
NR<=LINEMAX) print $0}' cru_ts_3_10.1901.2009.tmp.dat >> $datafile

year=$(($year+1))

done

#
#-------------------------------------------------------------------------------
# CHOOSE PLACES TO EXTRACT DATA

echo -e "\n******** FILTERING BY PLACE ********\n"

# X values: from 1-720
# Henry source zone: 541-580
# Henry Zoonosis zone: 489-534
xmin=541
xmax=580

# Y values: from 1-360
# Henry source zone: 241-260
# Henry Zoonosis zone: 257-276
ymin=241
ymax=260

datafile2=year"$yearmin"-"$yearmax"_month"$monthmin"-"$monthmax"_X"$xmin"-
"$xmax"_Y"$ymin"-"$ymax".dat

# Total number of months in datafile
nummonths=`echo "$monthmin $monthmax $yearmin $yearmax" | awk '{print (($2-
$1)+1)*(($4-$3)+1)}'`

# Creating loop to extract selected place for each month (each 360 lines)
month=1

rm $datafile2

while [[ $month -le $nummonths ]]
do

monthlinestart=`echo "$month $lpm" | awk '{print 1+(($1-1)*$2)}'`

monthlineend=`echo "$line1 $lpm" | awk '{print $1+$2}'`

yline1=`echo "$monthlinestart $ymin" | awk '{print $1+($2-1)}'`
yline2=`echo "$monthlinestart $ymax" | awk '{print $1+($2-1)}'`

echo "*** MONTH_NUMBER = $month *** Line numbers: monthstart=$monthlinestart
monthend=$monthlineend Ywindowstart=$yline1 Ywindowend=$yline2"

awk -v LINE1=$yline1 -v LINE2=$yline2 '{if (NR>=LINE1 && NR<=LINE2) print $0}'
$datafile | awk -v COL1=$xmin -v COL2=$xmax '{for(i=COL1;i<=COL2;++i) print $i}' >>
$datafile2
```

```
month=$(($month+1))

done

#
#-------------------------------------------------------------------------------
# CALCULATING AVERAGE FOR TIME/PLACE WINDOW

resultsfile=AVERAGE_year"$yearmin"-"$yearmax"_month"$monthmin"-
"$monthmax"_X"$xmin"-"$xmax"_Y"$ymin"-"$ymax".dat

mean=`awk -v SCALE=$scalar '{if ($1!=-999) sum+=$1; if ($1!=-999) n++} END {print
(sum/n)*SCALE}' $datafile2`

# Calculating standard deviation & standard error & writing out to results file

awk -v MEAN=$mean -v SCALE=$scalar '{if ($1!=-999) print (($1*SCALE)-MEAN)^2}'
$datafile2 | awk -v MEAN=$mean '{sum+=$1; n++} END {if (n>0) print "MEAN_AVG=",
MEAN, "NUM_DATAPOINTS=", n, "STAN_DEV=", ((sum/(n-1))^(1/2)), "STAN_ERR=",
((sum/(n-1))^(1/2))/(sqrt(n))}'  > $resultsfile
```

Supplementary Figure 1. Time series of area-averaged source region erythemal daily dose date through July 2011 illustrating peak surface UV-B radiation on July 4th. Produced using Nasa Giovanni environment (Data source, Hovila et al., 2013[108]).

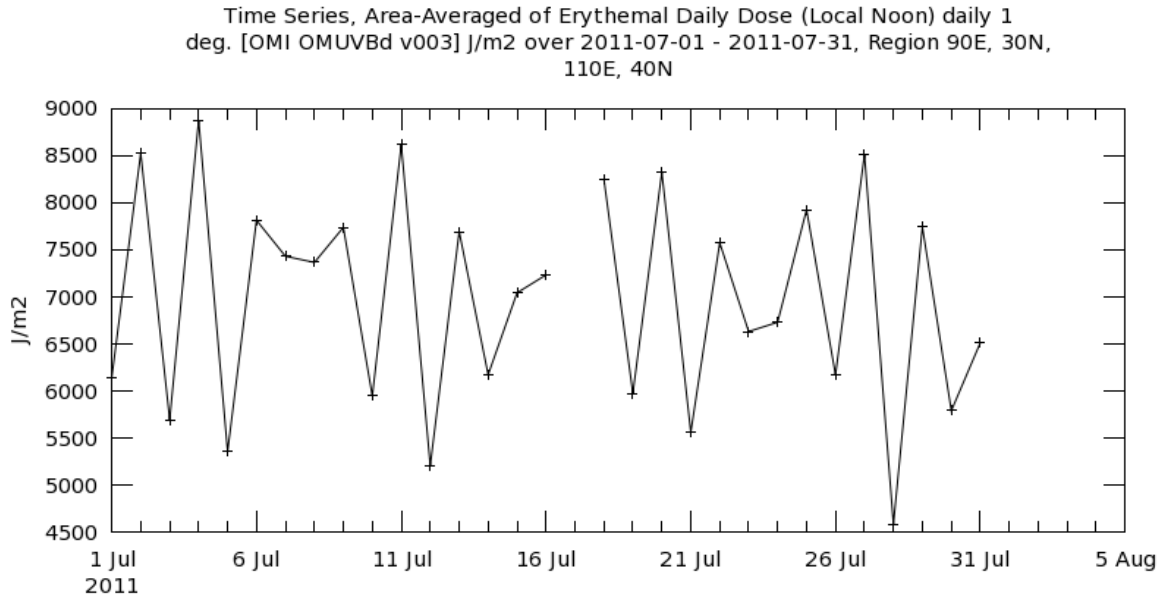

Supplementary Figure 2. Time averaged erythemal daily dose UV plot across the whole Himalayan region illustrating peak values within the source area as well as at higher altitudes proximal to Mount Everest.

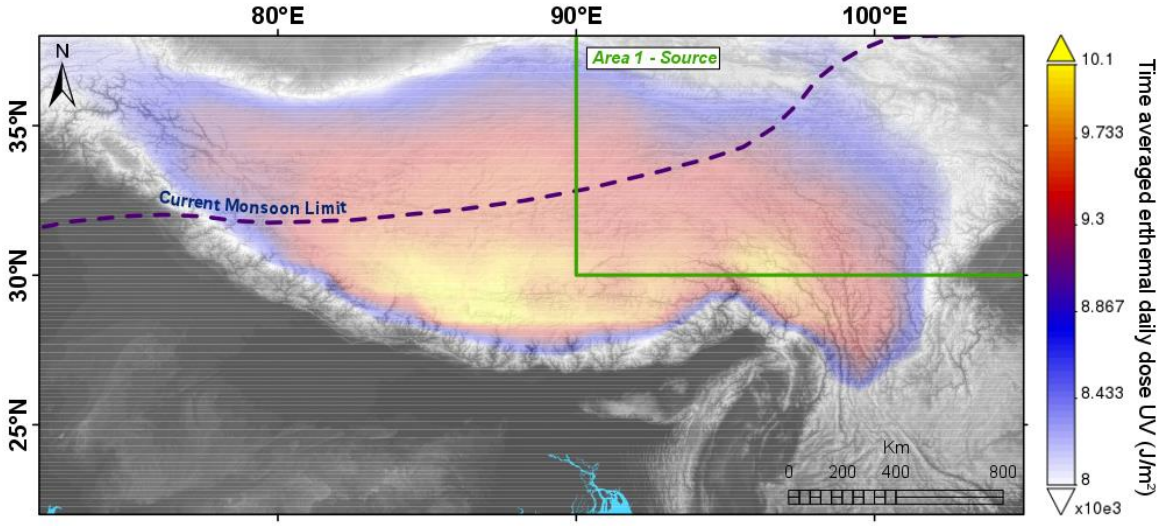

Supplementary Figure 3. Comparison of Asian temperature reconstructions across the period of cooling following volcanic loading of the early nineteenth century.

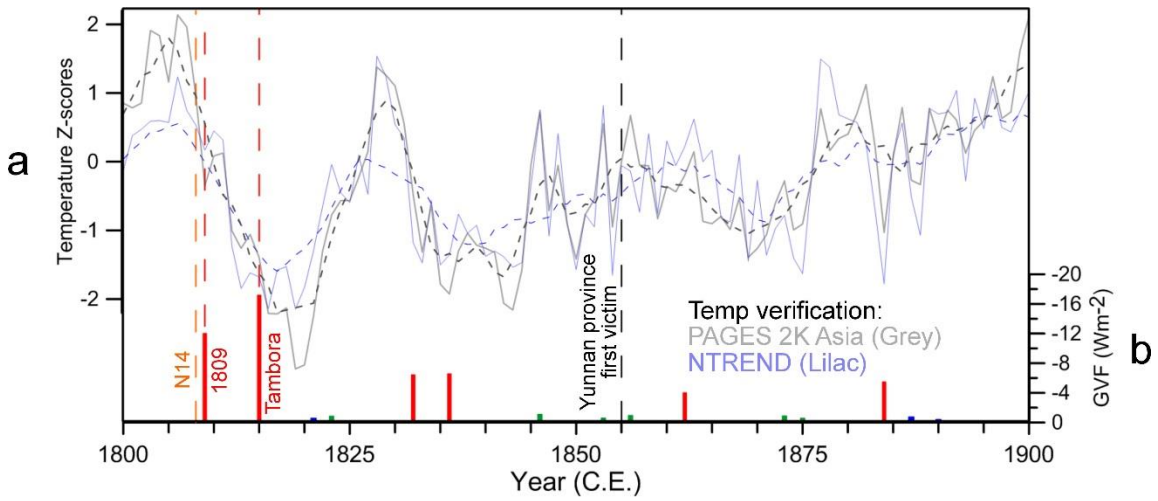

(**a**) Comparison of PAGES Asia 2K summer temperature reconstruction[61] with the N-TREND Northern Hemisphere summer temperature reconstruction for Eastern Eurasia[63] accompanied by eleven year running average values (dashed). (**b**) Global volcanic forcing estimates[44] separated by eruption latitude; southern hemisphere (blue), Northern Hemisphere (green) and tropical (red). The dates highlighted by dashed lines are; 1809 C.E. unknown eruption and the 1815 C.E. Tambora eruption (red), 1808 C.E. N14 polytomy[22] (Orange) and the 1855 C.E. estimated start date of the Third Pandemic within human populations[15] (Black).

Bibliography

1 Rosen, W. *Justinian's flea: plague, empire and the birth of Europe*. (Random House, 2010).

2 Green, M. H. *et al.* TMG 1 (2014): Pandemic Disease in the Medieval World: Rethinking the Black Death, ed. Monica Green. (2014).

3 Campbell, B. M. S. *The great transition : climate, disease and society in the late medieval world (2013 Ellen Mcarthur Lectures)*. (Cambridge University Press, 2016).

4 Stenseth, N. C. *et al.* Plague: past, present, and future. *PLoS Med* **5**, e3 (2008).

5 Kausrud, K. L. *et al.* Modeling the epidemiological history of plague in Central Asia: palaeoclimatic forcing on a disease system over the past millennium. *Bmc Biology* **8**, 112 (2010).

6 Ayyadurai, S., Sebbane, F., Raoult, D. & Drancourt, M. Body lice, Yersinia pestis orientalis, and black death. *Emerging infectious diseases* **16**, 892 (2010).

7 Dennis, D. T. *et al.* Plague manual: epidemiology, distribution, surveillance and control. (1999).

8 Kugeler, K. J., Staples, J. E., Hinckley, A. F., Gage, K. L. & Mead, P. S. Epidemiology of human plague in the United States, 1900–2012. *Emerging infectious diseases* **21**, 16 (2015).

9 WHO. *Plague*, <http://www.who.int/mediacentre/factsheets/fs267/en/> (2017).

10 Sebbane, F., Jarrett, C. O., Gardner, D., Long, D. & Hinnebusch, B. J. Role of the Yersinia pestis plasminogen activator in the incidence of distinct septicemic and bubonic forms of flea-borne plague. *Proceedings of the National Academy of Sciences* **103**, 5526-5530 (2006).

11 Prentice, M. B. & Rahalison, L. Plague. *The Lancet* **369**, 1196-1207 (2007).

12 Zimbler, D. L., Schroeder, J. A., Eddy, J. L. & Lathem, W. W. Early emergence of *Yersinia pestis* as a severe respiratory pathogen. *Nature Communications* **6** (2015).

13 Lathem, W. W., Crosby, S. D., Miller, V. L. & Goldman, W. E. Progression of primary pneumonic plague: a mouse model of infection, pathology, and bacterial transcriptional activity. *Proceedings of the National Academy of Sciences of the United States of America* **102**, 17786-17791 (2005).

14 Echenberg, M. J. Pestis redux: The initial years of the third bubonic plague pandemic, 1894-1901. *Journal of World History* **13**, 429-449 (2002).

15 Pollitzer, R. Plague. WHO Monograph Series 22. *World Health Organization, Geneva, Switzerland* (1954).

16 Stathakopoulos, D. C. *Famine and pestilence in the late Roman and early Byzantine empire: a systematic survey of subsistence crises and epidemics*. (Routledge, 2017).

17 Stewart, J. *Nestorian Missionary Enterprise: the story of a Church on fire*. (T. & T. Clark, 1928).

18 Kelly, J. The great mortality: An intimate history of the Black Death. (2006).

19 Bos, K. I. *et al.* A draft genome of Yersinia pestis from victims of the Black Death. *Nature* **478**, 506-510 (2011).

20 Bos, K. I. *et al.* Eighteenth century Yersinia pestis genomes reveal the long-term persistence of an historical plague focus. *Elife* **5**, e12994 (2016).

21 Rasmussen, S. *et al.* Early divergent strains of *Yersinia pestis* in Eurasia 5,000 years ago. *Cell* **163**, 571-582 (2015).

22 Cui, Y. *et al.* Historical variations in mutation rate in an epidemic pathogen, Yersinia pestis. *Proceedings of the National Academy of Sciences* **110**, 577-582 (2013).

23 Wagner, D. M. *et al.* Yersinia pestis and the Plague of Justinian 541–543 AD: a genomic analysis. *The Lancet Infectious Diseases* **14**, 319-326 (2014).

24 McMichael, A. J. Insights from past millennia into climatic impacts on human health and survival. *Proceedings of the National Academy of Sciences* **109**, 4730-4737 (2012).

25 Morelli, G. *et al.* Yersinia pestis genome sequencing identifies patterns of global phylogenetic diversity. *Nature genetics* **42**, 1140-1143 (2010).

26 Cliff, A., Smallman-Raynor, M., Haggett, P., Stroup, D. & Thacker, S. Emergence and re-emergence. Infectious diseases: a geographical analysis. *Emergence and re-emergence. Infectious diseases: a geographical analysis.* (2009).
27 Li, Y. *et al.* Genotyping and phylogenetic analysis of Yersinia pestis by MLVA: insights into the worldwide expansion of Central Asia plague foci. *PloS one* **4**, e6000 (2009).
28 Davis, S. *et al.* Predictive thresholds for plague in Kazakhstan. *Science* **304**, 736-738 (2004).
29 Kausrud, K. L. *et al.* Climatically driven synchrony of gerbil populations allows large-scale plague outbreaks. *Proceedings of the Royal Society of London B: Biological Sciences* **274**, 1963-1969 (2007).
30 Stenseth, N. C. *et al.* Plague dynamics are driven by climate variation. *Proceedings of the National Academy of Sciences* **103**, 13110-13115 (2006).
31 Ari, T. B. *et al.* Human plague in the USA: the importance of regional and local climate. *Biology letters* **4**, 737-740 (2008).
32 Collinge, S. K. *et al.* Testing the generality of a trophic-cascade model for plague. *EcoHealth* **2**, 102-112 (2005).
33 Schmid, B. V. *et al.* Climate-driven introduction of the Black Death and successive plague reintroductions into Europe. *Proceedings of the National Academy of Sciences* **112**, 3020-3025 (2015).
34 Wood, G. D. A. *Tambora: the eruption that changed the world*. (Princeton University Press, 2014).
35 Ambrose, S. H. Late Pleistocene human population bottlenecks, volcanic winter, and differentiation of modern humans. *Journal of Human Evolution* **34**, 623-651 (1998).
36 Gao, Y. & Gao, C. European hydroclimate response to volcanic eruptions over the past nine centuries. *International Journal of Climatology* (2017).
37 Stothers, R. B. Volcanic dry fogs, climate cooling, and plague pandemics in Europe and the Middle East. *Climatic change* **42**, 713-723 (1999).
38 Stothers, R. B. Climatic and demographic consequences of the massive volcanic eruption of 1258. *Climatic Change* **45**, 361-374 (2000).
39 Guillet, S. *et al.* Climate response to the Samalas volcanic eruption in 1257 revealed by proxy records. *Nature Geoscience* **10**, 123-128 (2017).
40 Huhtamaa, H. & Helama, S. Distant impact: tropical volcanic eruptions and climate-driven agricultural crises in seventeenth-century Ostrobothnia, Finland. *Journal of Historical Geography* **57**, 40-51 (2017).
41 Oppenheimer, C. Climatic, environmental and human consequences of the largest known historic eruption: Tambora volcano (Indonesia) 1815. *Progress in physical geography* **27**, 230-259 (2003).
42 Schaible, U. E. & Stefan, H. Malnutrition and infection: complex mechanisms and global impacts. *PLoS medicine* **4**, e115 (2007).
43 Büntgen, U. *et al.* Cooling and societal change during the Late Antique Little Ice Age from 536 to around 660 AD. *Nature Geoscience* **9**, 231-236 (2016).
44 Sigl, M. *et al.* Timing and climate forcing of volcanic eruptions for the past 2,500 years. *Nature* **523**, 543-549 (2015).
45 Miller, G. H. *et al.* Abrupt onset of the Little Ice Age triggered by volcanism and sustained by sea-ice/ocean feedbacks. *Geophysical Research Letters* **39** (2012).
46 Keys, D. *Catastrophe: an investigation into the origins of the modern world*. (Ballantine Books, 2000).
47 Stoffel, M. *et al.* Estimates of volcanic-induced cooling in the Northern Hemisphere over the past 1,500 years. *Nature Geoscience* (2015).
48 Brasseur, G. & Granier, C. Mount Pinatubo aerosols, chlorofluorocarbons, and ozone depletion. *Science* **257**, 28 (1992).
49 Tabazadeh, A. & Turco, R. Stratospheric chlorine injection by volcanic eruptions: HCl scavenging and implications for ozone. *Science* **260**, 1082-1086 (1993).

50 Vogelmann, A., Ackerman, T. & Turco, R. Enhancements in biologically effective ultraviolet radiation following volcanic eruptions. *Nature* **359**, 47 (1992).
51 Solomon, S. *et al.* The role of aerosol variations in anthropogenic ozone depletion at northern midlatitudes. *Journal of Geophysical Research: Atmospheres* **101**, 6713-6727 (1996).
52 Kerr, J. & McElroy, C. Evidence for large upward trends of ultraviolet-B radiation linked to ozone depletion. *Science(Washington)* **262**, 1032-1034 (1993).
53 Beckmann, M. *et al.* glUV: a global UV-B radiation data set for macroecological studies. *Methods in Ecology and Evolution* **5**, 372-383 (2014).
54 Beerling, D. J., Harfoot, M., Lomax, B. & Pyle, J. A. The stability of the stratospheric ozone layer during the end-Permian eruption of the Siberian Traps. *Philosophical Transactions of the Royal Society of London A: Mathematical, Physical and Engineering Sciences* **365**, 1843-1866 (2007).
55 Willis, K., Bennett, K. & Birks, H. Variability in thermal and UV-B energy fluxes through time and their influence on plant diversity and speciation. *Journal of Biogeography* **36**, 1630-1644 (2009).
56 Murphy, B. R. & Mitchell, F. J. An association between past levels of ozone column depletion and abnormal pollen morphology in the model angiosperm Arabidopsis thaliana L. *Review of Palaeobotany and Palynology* **194**, 12-20 (2013).
57 Flenley, J. Ultraviolet insolation and the tropical rainforest: Altitudinal variations, Quaternary and recent change, extinctions, and biodiversity. *Tropical rainforest responses to climatic change*, 219-235 (2007).
58 Cui, Y. *et al.* Historical variations in mutation rate in an epidemic pathogen, *Yersinia pestis*. *Proceedings of the National Academy of Sciences USA* **110**, 577-582, doi:10.1073/pnas.1205750110 (2013).
59 Maddison, W. P. Gene trees in species trees. *Systematic biology* **46**, 523-536 (1997).
60 Stenseth, N. C. *et al.* Plague dynamics are driven by climate variation. *Proceedings of the National Academy of Sciences USA* **103**, 13110-13115 (2006).
61 Cook, E. R. *et al.* Tree-ring reconstructed summer temperature anomalies for temperate East Asia since 800 CE. *Climate Dynamics* **41**, 2957-2972 (2013).
62 Cook, E. R. *et al.* Asian monsoon failure and megadrought during the last millennium. *Science* **328**, 486-489 (2010).
63 Wilson, R. *et al.* Last millennium northern hemisphere summer temperatures from tree rings: Part I: The long term context. *Quaternary Science Reviews* **134**, 1-18 (2016).
64 Inglesby, T. V. *et al.* Plague as a biological weapon: medical and public health management. *Jama* **283**, 2281-2290 (2000).
65 Galimand, M., Carniel, E. & Courvalin, P. Resistance of Yersinia pestis to antimicrobial agents. *Antimicrobial agents and chemotherapy* **50**, 3233-3236 (2006).
66 Rajanna, C. *et al.* A strain of Yersinia pestis with a mutator phenotype from the Republic of Georgia. *FEMS microbiology letters* **343**, 113-120 (2013).
67 Yan, Y. *et al.* Two-step source tracing strategy of Yersinia pestis and its historical epidemiology in a specific region. *PloS one* **9**, e85374 (2014).
68 Spyrou, M. A. *et al.* Historical Y. pestis genomes reveal the European black death as the source of ancient and modern plague pandemics. *Cell host & microbe* **19**, 874-881 (2016).
69 Papagrigorakis, M. J., Yapijakis, C., Synodinos, P. N. & Baziotopoulou-Valavani, E. DNA examination of ancient dental pulp incriminates typhoid fever as a probable cause of the Plague of Athens. *International Journal of Infectious Diseases* **10**, 206-214 (2006).
70 Manley, J. Measles and ancient plagues: a note on new scientific evidence. *Classical World* **107**, 393-397 (2014).
71 Drummond, A. J. & Rambaut, A. BEAST: Bayesian evolutionary analysis by sampling trees. *BMC evolutionary biology* **7**, 214 (2007).
72 Benton, M., Donoghue, P. & Asher, R. Calibrating and constraining molecular clocks. *The timetree of life*, 35-86 (2009).

73 Runnegar, B. A molecular-clock date for the origin of the animal phyla. *Lethaia* **15**, 199-205 (1982).
74 Tsubokura, M. *et al.* Special features of distribution of Yersinia pseudotuberculosis in Japan. *Journal of clinical microbiology* **27**, 790-791 (1989).
75 Gage, K. L. & Kosoy, M. Y. Natural history of plague: perspectives from more than a century of research. *Annu. Rev. Entomol.* **50**, 505-528 (2005).
76 Cash, R. A. & Narasimhan, V. Impediments to global surveillance of infectious diseases: consequences of open reporting in a global economy. *Bulletin of the World Health Organization* **78**, 1358-1367 (2000).
77 Galimand, M. *et al.* Multidrug resistance in Yersinia pestis mediated by a transferable plasmid. *New England Journal of Medicine* **337**, 677-681 (1997).
78 Guiyoule, A. *et al.* Transferable plasmid-mediated resistance to streptomycin in a clinical isolate of Yersinia pestis. *Emerging infectious diseases* **7**, 43 (2001).
79 Morgan, D., Allen, J. & di Cosmo, P. The Cambridge History of Inner Asia. The Chinggisid Age. *Bulletin of the School of Oriental and African Studies. University of London* **73**, 330 (2010).
80 Kool, J. L. & Weinstein, R. A. Risk of person-to-person transmission of pneumonic plague. *Clinical Infectious Diseases* **40**, 1166-1172 (2005).
81 Hinnebusch, B. J., Chouikha, I. & Sun, Y.-C. Ecological Opportunity, Evolution, and the Emergence of Flea-Borne Plague. *Infection and immunity* **84**, 1932-1940 (2016).
82 Sun, Y.-C., Jarrett, C. O., Bosio, C. F. & Hinnebusch, B. J. Retracing the evolutionary path that led to flea-borne transmission of Yersinia pestis. *Cell host & microbe* **15**, 578-586 (2014).
83 Chouikha, I. & Hinnebusch, B. J. Yersinia–flea interactions and the evolution of the arthropod-borne transmission route of plague. *Current opinion in microbiology* **15**, 239-246 (2012).
84 Bibikova, V., Il'inskaya, V., Kaluzhenova, Z., Morozova, I. & Shmuter, M. On biology of the Xenopsylla fleas in the Sary-Eshikotrau desert. *Zool. J. Moscow* **42**, 1045-1051 (1963).
85 Park, S. *et al.* Statistical analysis of the dynamics of antibody loss to a disease-causing agent: plague in natural populations of great gerbils as an example. *Journal of the Royal Society Interface* **4**, 57-64 (2007).
86 Büntgen, U., Ginzler, C., Esper, J., Tegel, W. & McMichael, A. J. Digitizing historical plague. *Clinical infectious diseases* **55**, 1586-1588 (2012).
87 Mitchell, S. *A history of the later Roman Empire, AD 284-641*. (John Wiley & Sons, 2014).
88 Büntgen, U. *et al.* 2500 years of European climate variability and human susceptibility. *Science* **331**, 578-582 (2011).
89 Keeling, M. & Gilligan, C. Metapopulation dynamics of bubonic plague. *Nature* **407**, 903-906 (2000).
90 Horrox, R. *The black death*. Vol. 1 (Manchester University Press, 1994).
91 Scott, S. & Duncan, C. J. *Biology of plagues: evidence from historical populations*. (Cambridge University Press, 2001).
92 Morgan, D. The decline and fall of the Mongol Empire. *Journal of the Royal Asiatic Society* **19**, 427-437 (2009).
93 Kakar, H. K. *Government and Society in Afghanistan: The Reign of Amir 'Abd al-Rahman Khan*. Vol. 5 (University of Texas Press, 2011).
94 Putnam, A. E. *et al.* Little Ice Age wetting of interior Asian deserts and the rise of the Mongol Empire. *Quaternary Science Reviews* **131**, 33-50 (2016).
95 Dols, M. W. *The Black Death in the Middle East*. (Princeton University Press, Guildford, Surrey., 1977).
96 Amitai, R. & Biran, M. Mongols, Turks and others: Eurasian nomads and the sedentary world. (2004).
97 DeWitte, S. & Slavin, P. Between famine and death: England on the eve of the Black Death—evidence from paleoepidemiology and manorial accounts. *Journal of Interdisciplinary History* **44**, 37-60 (2013).

98 Hymes, R. Epilogue: a hypothesis on the East Asian beginnings of the Yersinia pestis polytomy. *The Medieval Globe* **1**, 12 (2016).
99 More, A. F. *et al.* Next generation ice core technology reveals true minimum natural levels of lead (Pb) in the atmosphere: insights from the Black Death. *GeoHealth* (2017).
100 Borsch, S. Plague depopulation and irrigation decay in Medieval Egypt. *The Medieval Globe* **1**, 7 (2016).
101 Varlık, N. New science and old sources: why the Ottoman experience of plague matters. *The Medieval Globe* **1**, 9 (2016).
102 Khan, I. A. Plague: the dreadful visitation occupying the human mind for centuries. *Transactions of the Royal Society of Tropical Medicine and Hygiene* **98**, 270-277 (2004).
103 Atwill, D. G. Blinkered Visions: Islamic Identity, Hui Ethnicity, and the Panthay Rebellion in Southwest China, 1856—1873. *The Journal of Asian Studies* **62**, 1079-1108 (2003).
104 Zhang, Z. *et al.* Periodic climate cooling enhanced natural disasters and wars in China during AD 10–1900. *Proceedings of the Royal Society of London B: Biological Sciences*, rspb20100890 (2010).
105 Hanjra, M. A. & Qureshi, M. E. Global water crisis and future food security in an era of climate change. *Food Policy* **35**, 365-377 (2010).
106 Neerinckx, S., Bertherat, E. & Leirs, H. Human plague occurrences in Africa: an overview from 1877 to 2008. *Transactions of the Royal Society of Tropical Medicine and Hygiene* **104**, 97-103 (2010).
107 Chen, F.-H. *et al.* Moisture changes over the last millennium in arid central Asia: a review, synthesis and comparison with monsoon region. *Quaternary Science Reviews* **29**, 1055-1068 (2010).
108 Jari Hovila, A. A., and Johanna Tamminen. (NASA Goddard Space Flight Center, Goddard Earth Sciences Data and Information Services Center (GES DISC), 2013).
109 Investigator, I. T. P. I. P. L. K. C.-P. I. J. T. F. D. P. *OMI - Aura*, <https://aura.gsfc.nasa.gov/omi.html> (2016).
110 R: A Language and Environment for Statistical Computing (2016).
111 ncdf4: Interface to Unidata netCDF (Version 4 or Earlier) Format Data Files (2017).
112 (EROS), U. S. G. S. s. C. f. E. R. O. a. S. (1996).
113 University of East Anglia Climatic Research Unit; Jones, P. D. H., I.C. (NCAS British Atmospheric Data Centre, 2013).
114 Raoult, D. & Drancourt, M. in *Paleomicrobiology* 145-159 (Springer, 2008).
115 Seifert, L. *et al.* Genotyping Yersinia pestis in Historical Plague: Evidence for Long-Term Persistence of Y. pestis in Europe from the 14th to the 17th Century. *PLoS One* **11**, e0145194 (2016).
116 Alfani, G. Plague in seventeenth-century Europe and the decline of Italy: an epidemiological hypothesis. *European Review of Economic History* **17**, 408-430 (2013).
117 Rodenwaldt, E. World Atlas of Epidemic Diseases. *World Atlas of Epidemic Diseases.* (1956).
118 Xu, L. *et al.* Nonlinear effect of climate on plague during the third pandemic in China. *Proceedings of the National Academy of Sciences* **108**, 10214-10219 (2011).
119 Rowan, A. V. The 'Little Ice Age'in the Himalaya: A review of glacier advance driven by Northern Hemisphere temperature change. *The Holocene* **27**, 292-308 (2017).
120 Armstrong, B. K. Stratospheric ozone and health. *International journal of epidemiology* **23**, 873-885 (1994).
121 Ries, G. *et al.* Elevated UV-B radiation reduces genome stability in plants. *Nature* **406**, 98-101 (2000).
122 Peak, M., Peak, J., Moehring, M. & Webs, R. Ultraviolet action spectra for DNA dimer induction, lethality, and mutagenesis in Escherichia coli with emphasis on the UVB region. *Photochemistry and photobiology* **40**, 613-620 (1984).
123 Hansen, V. *The Silk Road: A New History*. (Oxford University Press, 2012).

124 Liu, X. in *The Cambridge World History: Volume IV: A World with States, Empires and Networks 1200 BCE–900 CE* Vol. IV (ed C. Benjamin) 435–456 (Cambridge University Press (The Cambridge World History), 2015).
125 Aryal, A. *et al.* Habitat, diet, macronutrient, and fiber balance of Himalayan marmot (Marmota himalayana) in the Central Himalaya, Nepal. *Journal of Mammalogy* **96**, 308-316 (2015).
126 Robock, A. Volcanic eruptions and climate. *Reviews of Geophysics* **38**, 191-219 (2000).
127 Mather, T. A. Volcanoes and the environment: Lessons for understanding Earth's past and future from studies of present-day volcanic emissions. *Journal of Volcanology and Geothermal Research* **304**, 160-179 (2015).
128 Eric Klobas, J., Wilmouth, D. M., Weisenstein, D. K., Anderson, J. G. & Salawitch, R. J. Ozone depletion following future volcanic eruptions. *Geophysical Research Letters*, n/a-n/a, doi:10.1002/2017GL073972.
129 McCormick, M. P., Thomason, L. W. & Trepte, C. R. Atmospheric effects of the Mt Pinatubo eruption. *Nature* **373**, 399 (1995).
130 Telford, P., Braesicke, P., Morgenstern, O. & Pyle, J. Reassessment of causes of ozone column variability following the eruption of Mount Pinatubo using a nudged CCM. *Atmospheric Chemistry and Physics* **9**, 4251-4260 (2009).
131 Herman, J., Bhartia, P., Ziemke, J., Ahmad, Z. & Larko, D. UV-B increases (1979–1992) from decreases in total ozone. *Geophysical Research Letters* **23**, 2117-2120 (1996).
132 Feister, U., Jäkel, E. & Gericke, K. Parameterization of daily solar global ultraviolet irradiation. *Photochemistry and photobiology* **76**, 281-293 (2002).
133 Montzka, S. *et al.* Scientific assessment of ozone depletion: 2010. *Global Ozone Research and Monitoring Project-Report No. 51* (2011).
134 Timmreck, C. Modeling the climatic effects of large explosive volcanic eruptions. *Wiley Interdisciplinary Reviews: Climate Change* **3**, 545-564 (2012).
135 Montzka, S. A. *et al.* Decline in the tropospheric abundance of halogen from halocarbons: Implications for stratospheric ozone depletion. *Science*, 1318-1322 (1996).
136 Daniel, J., Solomon, S., Portmann, R. & Garcia, R. Stratospheric ozone destruction: The importance of bromine relative to chlorine. *Journal of Geophysical Research: Atmospheres* **104**, 23871-23880 (1999).
137 Gerlach, T. M., Westrich, H. R. & Symonds, R. B. Preeruption vapor in magma of the climactic Mount Pinatubo eruption: Source of the giant stratospheric sulfur dioxide cloud. *Fire and mud: eruptions and lahars of Mount Pinatubo, Philippines* **415**, 33 (1996).
138 Tupper, A., Oswalt, J. S. & Rosenfeld, D. Satellite and radar analysis of the volcanic-cumulonimbi at Mount Pinatubo, Philippines, 1991. *Journal of Geophysical Research: Atmospheres* **110** (2005).
139 Carn, S., Clarisse, L. & Prata, A. Multi-decadal satellite measurements of global volcanic degassing. *Journal of Volcanology and Geothermal Research* **311**, 99-134 (2016).
140 Cadoux, A., Scaillet, B., Bekki, S., Oppenheimer, C. & Druitt, T. H. Stratospheric ozone destruction by the bronze-age Minoan eruption (Santorini volcano, Greece). *Scientific Reports* **5** (2015).
141 Vidal, C. M. *et al.* The 1257 Samalas eruption (Lombok, Indonesia): the single greatest stratospheric gas release of the Common Era. *Scientific reports* **6**, 34868 (2016).
142 Lavigne, F. *et al.* Source of the great AD 1257 mystery eruption unveiled, Samalas volcano, Rinjani Volcanic Complex, Indonesia. *Proceedings of the National Academy of Sciences* **110**, 16742-16747 (2013).
143 Paladio-Melosantos, M. L. O. *et al.* Tephra falls of the 1991 eruptions of Mount Pinatubo. *Fire and mud* **12000**, 12030 (1996).
144 Jousset, P. *et al.* The 2010 explosive eruption of Java's Merapi volcano—a '100-year'event. *Journal of volcanology and geothermal research* **241**, 121-135 (2012).
145 Zuev, V., Zueva, N., Savelieva, E., Bazhenov, O. & Nevzorov, A. On the role of the eruption of the Merapi volcano in an anomalous total ozone decrease over Tomsk in April 2011. *Atmospheric and Oceanic Optics* **29**, 298-303 (2016).

146 Guo, S., Bluth, G. J., Rose, W. I., Watson, I. M. & Prata, A. Re-evaluation of SO2 release of the 15 June 1991 Pinatubo eruption using ultraviolet and infrared satellite sensors. *Geochemistry, Geophysics, Geosystems* **5** (2004).
147 Raible, C. C. *et al.* Tambora 1815 as a test case for high impact volcanic eruptions: Earth system effects. *Wiley Interdisciplinary Reviews: Climate Change* **7**, 569-589 (2016).
148 Zdanowicz, C. M., Zielinski, G. A. & Germani, M. S. Mount Mazama eruption: Calendrical age verified and atmospheric impact assessed. *Geology* **27**, 621-624 (1999).
149 Survey, S. I. a. U. G. Weekly Volcanic Activity Report, 3 November-9 November 2010. (Smithsonian Institution and US Geological Survey, Global Volcanism Program, 2010).
150 Petkov, B. H. *et al.* Response of the ozone column over Europe to the 2011 Arctic ozone depletion event according to ground-based observations and assessment of the consequent variations in surface UV irradiance. *Atmospheric environment* **85**, 169-178 (2014).
151 Qian, Q. *et al.* Mapping risk of plague in Qinghai-Tibetan Plateau, China. *BMC infectious diseases* **14**, 382 (2014).
152 GBIF Secretariat:. *GBIF Marmota himalayana (Hodgson, 1841)*, <https://www.gbif.org/species/2437371> (2017).
153 Gao, C., Robock, A. & Ammann, C. Volcanic forcing of climate over the past 1500 years: An improved ice core-based index for climate models. *Journal of Geophysical Research: Atmospheres* **113** (2008).
154 Crowley, T. J. & Unterman, M. B. Technical details concerning development of a 1200 yr proxy index for global volcanism. *Earth System Science Data* **5**, 187-197 (2013).
155 Lopez, A. D., Mathers, C. D., Ezzati, M., Jamison, D. T. & Murray, C. J. Global and regional burden of disease and risk factors, 2001: systematic analysis of population health data. *The Lancet* **367**, 1747-1757 (2006).
156 Christakos, G., Olea, R. A. & Yu, H.-L. Recent results on the spatiotemporal modelling and comparative analysis of Black Death and bubonic plague epidemics. *Public Health* **121**, 700-720 (2007).
157 Wang, Y.-J., Pan, J.-T., Liu, S.-W. & Liu, J.-Q. A new species of *Saussurea* (Asteraceae) from Tibet and its systematic position based on ITS sequence analysis. *Botanical Journal of the Linnean Society* **147**, 349-356 (2005).
158 Dashu, Q. in *Ancient Silk Trade Routes: Selected Works from Symposium on Cross Cultural Exchanges and Their Legacies in Asia.* 87 (World Scientific).
159 Semenza, J. C. & Menne, B. Climate change and infectious diseases in Europe. *The Lancet infectious diseases* **9**, 365-375 (2009).
160 Samia, N. I. *et al.* Dynamics of the plague–wildlife–human system in Central Asia are controlled by two epidemiological thresholds. *Proceedings of the National Academy of Sciences* **108**, 14527-14532 (2011).
161 Witter, J. & Self, S. The Kuwae (Vanuatu) eruption of AD 1452: potential magnitude and volatile release. *Bulletin of Volcanology* **69**, 301-318 (2007).
162 Rose, W. I. *et al.* Atmospheric chemistry of a 33–34 hour old volcanic cloud from Hekla Volcano (Iceland): Insights from direct sampling and the application of chemical box modeling. *Journal of Geophysical Research: Atmospheres* **111** (2006).
163 Walker, G. C. Mutagenesis and inducible responses to deoxyribonucleic acid damage in Escherichia coli. *Microbiological Reviews* **48**, 60 (1984).
164 Zenoff, V. F., Sineriz, F. & Farías, M. Diverse responses to UV-B radiation and repair mechanisms of bacteria isolated from high-altitude aquatic environments. *Applied and environmental microbiology* **72**, 7857-7863 (2006).
165 Ari, T. B. *et al.* Plague and climate: scales matter. *PLoS Pathogens* **7**, e1002160 (2011).
166 Snäll, T., O'Hara, R., Ray, C. & Collinge, S. Climate-driven spatial dynamics of plague among prairie dog colonies. *The American Naturalist* **171**, 238-248 (2007).
167 Nakazawa, Y. *et al.* Climate change effects on plague and tularemia in the United States. *Vector-borne and zoonotic diseases* **7**, 529-540 (2007).

168 Cassell, G. H. & Mekalanos, J. Development of antimicrobial agents in the era of new and reemerging infectious diseases and increasing antibiotic resistance. *Jama* **285**, 601-605 (2001).